NN 8201, 1025

CENTRALE LANDBOUWCATALOGUS
0000 0068 6135

THE PREPARATION AND STABILITY OF HOMODISPERSE COLLOIDAL HAEMATITE (α-Fe_2O_3)

BIBLIOTHEEK
LANDBOUWHOGESCHOOL
WAGENINGEN

Promotor: dr. J. Lyklema,
hoogleraar in de fysische en kolloïdchemie.

Co-promotor: dr. ir. L.K. Koopal,
wetenschappelijk hoofdmedewerker.

NN08201,1025

N.H.G. Penners

THE PREPARATION AND STABILITY OF HOMODISPERSE COLLOIDAL HAEMATITE (α-Fe_2O_3)

Pro ift

ter ijging van de graad van
doc de landbouwwetenschappen,
op van de rector magnificus,
dr. Oosterlee,
in enbaar te verdedigen
op g 15 maart 1985
des dags om half drie in de aula
va ndbouwhogeschool te Wageningen.

ISN-221048-03

NN08201, 1025

BIBLIOTHEEK L.H.

0 5 MAAR 1985

ONTV. TIJDSCHR. ADM.

ELLINGEN

Isaacson en medewerkers schrijven de afname van de ethyleendibromide (EDB) concentratie in verontreinigd grondwater ten onrechte toe aan azeotropische water-EDB mengsels.

Isaacson, P.J., Hankin,L. en Frink, C.R., Science, **225**, 672 (1984).

De conclusie van Eisenlauer en Matijević, dat de α-Fe_2O_3 deeltjes in hun hematiethydrosolen een polykristallijne structuur hebben, berust op een verkeerde interpretatie van de diffractiegegevens.

Eisenlauer, J. en Matijević, E., J. Colloid Interface Sci., **75**, 199 (1980).

Door geen rekening te houden met de directe redoxreactie tussen de redoxmediator N,N,N,N-tetramethylphenyleendiamide (TMPD) en zuurstof wordt vaak ten onrechte geconcludeerd dat TMPD boven bepaalde concentraties ontkoppelend op de eindademhaling werkt.

Krishnamoorthy, G. en Hinkle, P., Biochem. **23**, 1640 (1984).

De constante K_M in de formule van Manning, die wordt gebruikt voor de berekening van stroomsnelheden in waterlopen, is voor sommige sloten een debietgebonden variabele.

Bij de experimentele bepaling van het ladingsnulpunt kan men niet volstaan met potentiometrische titraties. Het resultaat dient door aanvullende electrokinetische metingen te worden geverifieerd.

Bij de selectie van gedoteerde keramische materialen voor toepassing in de electroden van hoge temperatuur brandstofcellen dient men de mate van afhankelijkheid tussen het electronisch geleidingsvermogen en de doteringsgraad als extra criterium te hanteren.

40951

7. De op verspreidingsberekeningen gebaseerde conclusie, dat de luchtkwaliteit in Midden-Limburg in belangrijke mate wordt bepa door het Ruhrgebied, is formeel gezien correct. Zij houdt echte niet in dat er m.b.t. de emissies door de PLEM centrales geen vuiltje aan de lucht is.

"De invloed van kolen stoken op de luchtkwaliteit in Midden-Limburg", Kema Rapport (1984).

8. De multilaterale uitwisseling van industrieel afval tussen de E lidstaten via lucht en water is eerder een uiting van nationaal egoisme dan van Europese geest.

9. In de discussies over de invloed van de zgn. "zure regen" op ecosystemen ziet men door de boom het bos niet meer.

10. Zwemmers in surfwater ervaren helaas maar al te vaak de dubbel betekenis van het woord "zwaard".

N.H.G. Penners
THE SYNTHESIS AND STABILITY OF HOMODISPERSE COLLOIDAL HAEMATITE (α-Fe_2O_3).
Wageningen, 15 maart 1985.

"Da steh' ich nun, ich armer Thor!,
und bin so klug, als wie zuvor..."

Johann Wolfgang von Goethe

CONTENTS

		page
I	INTRODUCTION	1
	1.1 General background of the study	1
	1.2 References	3
II	THE SYNTHESIS OF HOMODISPERSE HAEMATITE (α-Fe_2O_3) BY SEEDED GROWTH	5
	2.1 Abstract	5
	2.2 Introduction	5
	2.3 Experimental	6
	2.3.1 Materials	6
	2.3.2 Preparation of seed sol	7
	2.3.3 Seed sol purification	7
	2.3.4 Sol synthesis	7
	2.3.5 Iron concentration determination	8
	2.3.6 Electron microscopy	9
	2.3.7 Particle size	9
	2.3.8 Kinetic experiments	9
	2.4 Results	11
	2.4.1 Sols	11
	2.4.2 Growth kinetics	13
	2.5 Discussion	17
	2.6 Conclusions	20
	2.7 Acknowledgements	20
	2.8 References	21
III	TURBIDITY OF HOMODISPERSE HAEMATITE (α-Fe_2O_3) HYDROSOLS	24
	3.1 Abstract	24
	3.2 Introduction	24
	3.3 Experimental	25
	3.3.1 Haematite sols	25
	3.3.2 Concentration	25
	3.3.3 Turbidity measurements	25

3.3.4 Optical constants 25
3.3.5 Particle size and shape 26
3.3.6 Calculations 27
3.4 Results and discussion 28
3.5 Conclusions 31
3.6 Acknowledgements 31
3.7 References 31

IV INTERFACIAL ELECTROCHEMISTRY OF HAEMATITE 34
4.1 Abstract 34
4.2 Introduction 34
4.3 Experimental 36
4.3.1 Hydrosols 36
4.3.2 Specific surface area 36
4.3.3 Surface charge measurements 37
4.3.4 Streaming potential measurements 37
4.3.5 Coating of the capillary 38
4.3.6 Electrode 38
4.3.7 Electrophoresis 38
4.4 Results and discussion 39
4.4.1 Time effects and surface charge density 39
4.4.2 The common intersection point 42
4.4.3 Influence of heating 44
4.5 Conclusions 48
4.6 Acknowledgements 48
4.7 References 49

V THE EFFECT OF PARTICLE SIZE ON THE STABILITY OF HAEMATITE (α-Fe_2O_3) HYDROSOLS 51
5.1 Abstract 51
5.2 Introduction 51
5.2.1 General background 51
5.2.2 Basic aspects of colloid stability 53
5.3 Experiments and methods 58
5.3.1 Sols 58
5.3.2 Stability measurements 58
5.3.3 Turbidity data analysis 60

5.4 Results 61
5.4.1 Stability 61
5.4.2 Coagulation kinetics 64
5.5 Discussion 66
5.5.1 General considerations 66
5.5.2 Some geometrical considerations 72
5.6 Conclusions 76
5.7 References 77

VI GENERAL REFLECTIONS AND SUGGESTIONS FOR FURTHER RESEARCH 80
6.1 General 80
6.2 References 82

LIST OF ABBREVATIONS AND SYMBOLS 83

SUMMARY 86

SAMENVATTING 89

HINTERGRÜNDE DES PROMOTIONSTHEMAS 92

CURRICULUM VITAE 95

NAWOORD 96

The chapters II and III are submitted for publication in "Colloids and Surfaces."

INTRODUCTION

1.1 GENERAL BACKGROUND OF THE STUDY

Colloid stability, i.e. the stability of submicron particles against aggregation is a major problem point in the field of colloid chemistry. When in the forties Derjaguin and Landau [1] and Verwey and Overbeek [2] combined the concepts of van der Waals attraction and electrostatic repulsion between colloid particles in what is known as the DLVO theory, a framework was developed for the quantitative description of stability phenomena. The theory could explain many experimental trends, in particular the pronounced dependence of the critical coagulation concentration on counter ion valence, observed by Schulze and Hardy [3]. However, with regard to the influence of particle size on colloid stability, the theory was less successfull [3]. The expected stability increase with particle size has not been experimentally corroborated.

Partly this lack of experimental verification is due to experimental restrictions: In general, factors which influence the surface properties of a colloid, like surface charge, the occurence of specific adsorption and hydration, are the main stability determining parameters and size effects play only a subordinate part. In order to study particle size effects systematically, homodisperse sols must be available for a range of particle sizes at identical surface properties.

Due to such experimental restrictions, most of the size dependent experiments described in literature have been performed with perfectly spherical, homodisperse latices [4-7]. However, though this type of research did improve our understanding of the principles of stability, it too suffered from certain shortcomings: there is some evidence that the latex surface has a hairy structure [8,9] and therefore it does not meet the condition of a well-defined particle boundary required in appropriate model colloids. In addition, though their surface charge can be varied within certain limits, latices must be classified as low charged colloids [10] and consequently they are not characteristic for the many natural and industrial colloids which are highly charged.

It was the objective of the present Ph. D. project to contribute to the solution of the particle radius problem from an experimentally point of

view. In particular, the following aspects will be dealt with:

(a) The synthesis of suitable model systems, meeting the demands of homodispersity, sphericity, large particle size range and high surface charge density.
(b) The characterisation of the system with regard to optical and electrochemical properties. The obtained information provides the base for the turbidimetric monitoring of the coagulation processes and for the interpretation of the results in terms of double layer parameters.
(c) Investigation of the coagulation behaviour of differently sized particles, and comparsion of the results with the concepts of the DLVO theory.

Of the colloid systems encountered in nature and in technical applications, colloidal oxides in general, and ferric oxides in particular are of considerable importance. Iron oxides occur frequently as soil constituents [11], they are used on a large scale as pigments [12] and constitute the main products of corrosion processes [13]. Even in living organisms they play their part in the devices for magnetic navigation in certain magnetotactic bacteria as well as in higher organisms like dolphins and pigeons [14]. For such reasons iron oxides have been studied extensively for many years. As in addition they meet the condition of high surface charge, it was obvious to choose one of the representatives of the ferric (hydr)oxides as the model compound for the studies. In the department of Physical and Colloid chemistry of the Agricultural University Wageningen, early studies with α-Fe_2O_3 (haematite) [15] have lead to some know-how of its surface properties. Moreover, recent progress in the synthesis of morphologically well-defined haematite colloids [16] offered prospects for the development of α-Fe_2O_3 sols containing homodisperse spherical particles. Considering those facts, haematite was finally chosen as the model substance.

In **chapter 2**, a method is described for the synthesis of such homodisperse haematite sols with particle diameters ranging over a whole decade. To gain insight in the process of particle formation, the study has been extended by kinetic experiments.

Chapter 3 describes the optical characterisation of the haematite hydrosols obtained. The dependence of the turbidity of dilute sols on particle

size and wavelength is studied and experimental values are related to the light scattering theory for isotropic spheres (Mie theory). The studies are a prerequisite for the coagulation experiments described in chapter 5 as they provide the key for the conversion of turbidimetric data to kinetic parameters.

All stability phenomena are directly related to the electrochemical properties of the particle surface. The surface properties of haematite sols are studied in **chapter 4**, using potentiometric titration, electrophoresis and streaming potential measurements as the experimental tools.

The data and insights gained in the previous chapters are used in a study on the influence of particle size on colloidal stability, described in **chapter 5**.

Finally, **chapter 6** briefly reflects the possibilities and limits of the present study and points to problems deserving further elaboration as well as to means to make them experimentally accessible.

1.2 REFERENCES

(1) Derjaguin, B.V., and Landau, L.D., Acta Physicochim. URSS **14**, 633 (1941).

(2) Verwey, E.J.W., and Overbeek, J. Th.G., "The Theory of the Stability of Lyophobic Colloids", Elsevier, New York, Amsterdam (1948).

(3) Overbeek, J.Th.G., Advan. Colloid Interface Sci. **16**, 17 (1982).

(4) Matthews, B.A., and Rhodes, C.T., J. Colloid Interface Sci. **28**, 71 (1968).

(5) Watillon, A., and Joseph-Petit, A.M., Discuss. Faraday Soc. **42**, 143 (1966).

(6) Ottewil, R.H., and Shaw, J.N., Discuss. Faraday Soc. **42**, 154 (1966).

(7) Kotera, A., Furusawa, K., and Kudo, K., Kolloid - Z. Z. Polym. **240**, 837 (1970).

(8) van der Put, A., thesis, Agricultural University Wageningen, The Netherlands (1980).

(9) Bensley, C.N., and Hunter, R.J., J. Colloid Interface Sci. **92**, 448 (1983).

(10) Norde, W., thesis, Agricultural University Wageningen, The Netherlands (1976).

(11) Rooksby, H.P., in "The X-ray Identification and Crystal Structures of Clay Minerals", G. Brown Ed., Mineral Soc., London (1961).

(12) Lincke, G., Farbe Lack **75**, 632 (1969).

(13) Matijević, E., "Atmospheric Corrosion", Ailor, W.H., Ed., Wiley, New York, 123 (1982).

(14) Blakemore, R.P., and Frankel, R.B., Sci. Am. **245**, 42 (1981).

(15) Breeuwsma, A., thesis, Agricultural University Wageningen, The Netherlands (1973).

(16) Matijević, E., and Scheiner P., J. Colloid Interface Sci. **63**, 509 (1978).

II. THE SYNTHESIS OF HOMODISPERSE HAEMATITE (α-Fe_2O_3) SOLS BY SEEDED GROWTH

2.1 ABSTRACT

The principle of heterogeneous nucleation has been used to develop a method for preparation of homodisperse haematite (α-Fe_2O_3) sols with narrow size distributions over a wide range of diameters. Kinetic experiments, carried out at fixed supersaturation as well as under depleting conditions show that the precipitation is governed by a diffusion controlled incorporation of low molecular weight iron-hydroxy complexes in the solid phase. The particles formed are monocrystalline, and exhibit the crystallographic features of α-Fe_2O_3. Conditions which give rise to the formation of nearly spherical particles are very strict. Slight alterations in the reaction conditions may change the particle morphology significantly.

2.2 INTRODUCTION

Among the family of inorganic colloidal compounds, the ferric hydrous oxides are of special importance, partly because of their manifold appearance in nature as soil constituents and minerals, but also because of possible applications in industry. Their use as pigments, catalysts, coatings, fillers and in the production of magnetic tapes is widespread.

The formation of ferric hydrous oxides has been a subject of intensive research for more than 100 years [1-5]. However, in most reported cases, the prepared hydrosols were rather poorly defined with regard to their size and shape. Only few examples of relatively homodisperse systems are recorded [6-12].

It was the merit of Matijević and coworkers to extend the number of available homodisperse sols considerably. Their work covered metal hydrous oxides in general [13-20], and ferric compounds in particular [21-24]. The procedure generally applied in the synthesis was based on the principle of forced hydrolysis of homogeneous metal salt solutions under strictly defined conditions. It was shown that particle morphology, as well as size and appearance are influenced in a crucial way by the properties of the solvent [24,25], the concentration of the metallic compound, pH, temperature, and

the nature of the anion. Uniform, homodisperse particles are obtained only if these parameters are chosen in such a way that rapid homogeneous nucleation is followed by incorporation of the hydrolyzed metal species in the solid phase without formation of additional nuclei [18].

However simple the principle might be, its experimental realization is extremely difficult, as all conditions mentioned are in most cases very restrictive. A minor change in any of them might have drastic effects on the solid phase formed [21], and extensive cleaning precautions must be taken to exclude even trace amounts of impurities.

Some of the problems can be avoided, if the sols are prepared by heterogeneous rather than homogeneous nucleation, i.e. if the spontaneous additional formation of nuclei is suppressed. This method of seeded growth has been applied to a number of sparingly soluble substances [26-35], and kinetic expressions for the growth of seed crystals from solutions could be established. Analysis of the kinetics proved to be a powerful tool to monitor the condensation process and the mechanism of particle growth [34, 36].

In our search for the reproducible production of homodisperse haematite (α-Fe_2O_3) sols with spherical particles of variable diameter, we introduced the principle of seeded growth in the process of forced hydrolysis of ferric chloride solutions at elevated temperatures and established optimal conditions for the synthesis. Special attention has been paid to the kinetics of the precipitation process. Besides measuring the decrease of iron concentration with time we developed a method which enabled us to monitor the course of the reaction at constant supersaturation. A combination of both approaches proved to be suited to elucidate some basic aspects of particle growth.

2.3 EXPERIMENTAL

2.3.1 Materials

All chemicals were reagent grade, obtained from Merck or Baker, and used without further purification. Water was pre-purified by reversed osmosis and subsequently passed through a Millipore Super-Q system. Prior to use, all glassware was cleaned with concentrated hydrochloric acid, extensively rinsed with water, and finally steamed. Stock solutions of ferric chloride were prepared in high concentrations (2.6 M), to prevent hydrolysis

at room temperature. Solutions were passed through 0.22 micrometer Millipore filters in order to remove particulate contaminants. All glassware used (Duran, Pyrex) was made of borosilicate glass.

2.3.2 Preparation of seed sol

The seed sols, containing the smallest particles were prepared by a method essentially based on the procedure developed by Matijević and coworkers [21] for the synthesis of spherical particles with a modal diameter of 80–100 nm. The method was slightly modified to be suited for larger quantities of material: 25 ml of a solution, 0.72 M in $FeCl_3$ and 3.75×10^{-3} M in HCl, was mixed with 975 ml of preheated 3.75×10^{-3} M HCl in a 1 l Duran bottle resulting in a final concentration of 0.018 M $FeCl_3$ and 3.75×10^{-3} M HCl. During the mixing process, vigorous stirring was applied, to ensure immediate homogenisation of the mixture. Incubation was continued for 24 hours at 100°C ± 0,1°C in a Memmert forced convection oven to complete sol formation.

2.3.3 Seed sol purification

After incubation, the solutions were cooled to room temperature, and the sols coagulated by the addition of solid KCl up to a final concentration of 150 mM. After sedimentation of the flocs, the supernatant was discarded, the settled particles repeptisized in 10^{-3} M $HClO_4$ by ultrasonication and centrifuged in polycarbonate tubes at 8000 rpm. The procedure of centrifugation and redispersion was repeated several times. The appearance and the dispersity of the purified sol is illustrated in figures 1 and 2 (see results).

2.3.4 Sol synthesis

Larger batches of homodisperse sols with variable particle diameter have been prepared following this procedure: A 2 litre Duran bottle, containing 2000 ml of a solution, 5×10^{-3} M in $FeCl_3$ and 9×10^{-2} M in $HClO_4$, was incubated at 100°C ± 0.1°C in a Memmert forced convection oven. When the temperature reached 100°C, seed sol was injected. The reaction mixture was stirred by a magnetic stirrer to prevent settling of the sol. The desired particle size was obtained by selecting a suitable combination of nuclei size and nuclei concentration. Amounts of nuclei were chosen such, that 80% depletion was reached within 30 hours. Incubation times never exceeded 30 hours, and the maximum ratio between final radius and nucleus radius was set

to be three for one growth step. Every subsequent enlargement was achieved by using the grown sol as a seed sol in a following growth cycle. An example of conditions adapted in a typical growth sequence leading to particles with a radius of 282 nm is given in table 1. Sols were purified by repeated centrifugation in 10^{-3} M $HClO_4$ and decantation of the supernatant. To achieve an additional fractionation of the samples, the rate of sedimentation was adjusted to the particle size. In those cases where the particles were big enough, purification was carried out by gravitational sedimentation and subsequent removal of the supernatant. After purification, sols were stored in 10^{-3} M $HClO_4$. Before further use, the sols were subjected to an ultrasonic treatment to ensure redispersion of aggregates.

TABLE 1. CONDITIONS ADAPTED IN A TYPICAL GROWTH SEQUENCE

seed particle radius (r_0) (nm)	seed concentration (mg/l)	radius of growth product (nm)	r/r_0
34	49.9	73	2.1
34	14.8	95	2.8
73	49.9	134	1.8
95	77.9	172	1.8
134	101.5	213	1.6
172	154.5	253	1.5
213	186.0	282	1.3

2.3.5 Iron concentration determination

The concentration of free Fe^{3+} was determined, using a modification of the thiocyanate method, described by Vogel [37]. An aliquot of the sample was centrifuged in a table centrifuge to remove all solid iron compounds. 50 microlitre of the supernatant was subsequently added to a mixture of 4.15 ml water, 0.3 ml 4 M HNO_3 and 0.5 ml 2 M KSCN in a 14x100 mm pyrex tube. The optical density of the mixture was measured at 480 nm using a Beckman model 3600 spectrophotometer, and compared with a reference curve obtained with a series of standard solutions of $NH_4\ Fe(SO_4)_2.12H_2O$, ranging from 0 to 2 mg/ml.

2.3.6 Electron microscopy

Droplets of dilute sols in water were brought on to formvar-coated 200 mesh copper grids, and the particles were allowed to settle for some minutes. The settling time was adjusted to particle size. The excess solution was soaked off and the grids were dried at room temperature before being examined in a Philips T 400 electron microscope. Grids were covered with evaporated carbon prior to analysis to avoid charging and to stabilize the membrane.

2.3.7 Particle size

Size distributions were obtained by analyzing transmission electron microscope photographs with the aid of a Quantimet 720 particle-sizer. Individual projected particle areas were related to particle size by assuming spherical geometry. For every histogram, 300 particles were measured.

2.3.8 Kinetic experiments

(a) Depletion experiments: Experiments in which the decrease of the free iron concentration in solution was followed as a function of the incubation time, were carried out either in 14x100 mm Pyrex tubes (experiments under non stirring conditions) or in 250 ml Duran bottles (equipped with a magnetic stirrer in the cases when stirring was applied). At set times, samples of the reaction mixture were drawn, cooled to room temperature and centrifuged to remove the solid compounds. An aliquot of the supernatant was taken to determine the concentration of Fe^{3+}, using the thiocyanate method.

(b) Reactions at constant supersaturation: Growth experiments at constant iron and perchloric acid concentration were carried out by adding to the reaction fluid a solution containing $HClO_4$ and $FeCl_3$ in a fixed ratio, which is determined by the fact that haematite precipitation is governed by the following over all stoichiometry:

$$2\ Fe^{3+} + 3H_2O \longrightarrow Fe_2O_3 + 6H^+ \qquad (2.1)$$

That three protons are released for every disappearing Fe^{3+} ion has indeed been verified experimentally by measuring the pH as a function of the iron concentration in depletion reactions. The reaction was monitored by measuring the conductance of the reaction fluid. As soon as a preset value of the conductivity was surpassed, a home-made regulation unit caused a Mettler

model 655 automatic burette to add the iron and acid containing solution into the reaction vessel. Addition stopped when the conductivity and hence the concentrations of the reaction components reached their original values. The electrode used was made of two pieces of platinum wire, embedded in an all teflon design. The Pt wire was blackened, using the method of Ives and Janz [38]. This treatment appeared to be essential, as haematite precipitation proved to be a serious problem on non-blackened surfaces.

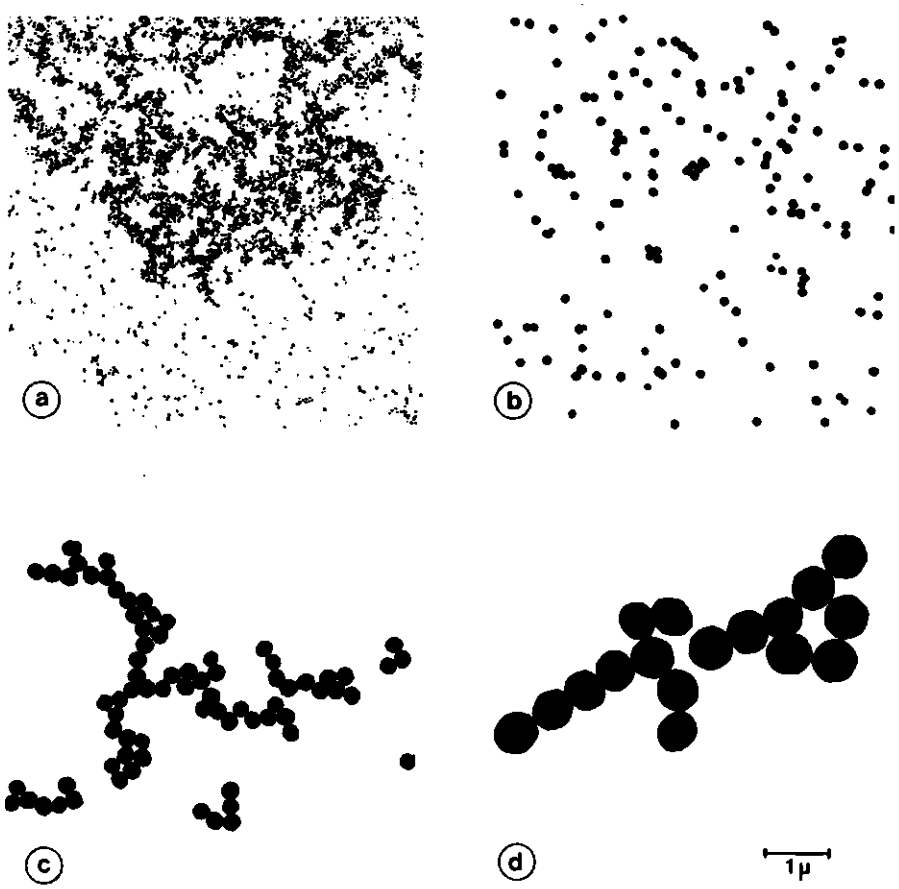

FIGURE 2.1. Transmission electron micrographs of some haematite samples, prepared by seeded growth. All images refer to the same magnification, indicated by the bar. Particles, used as primary seeds are exhibited in fig. a.

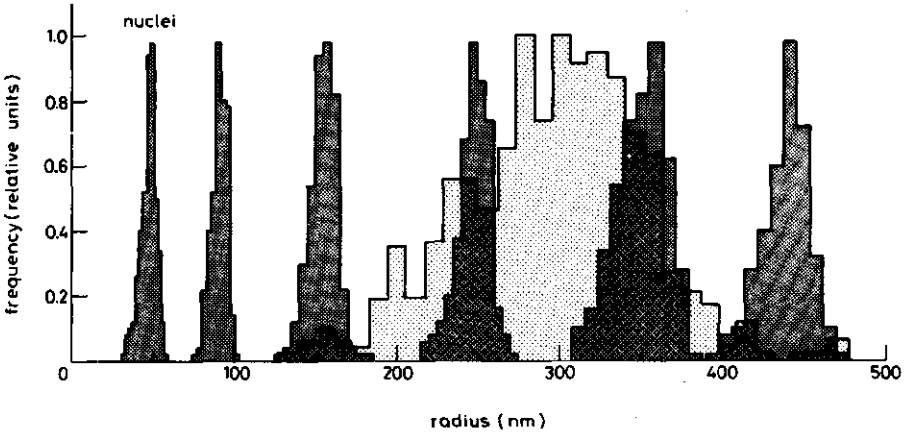

FIGURE 2.2. Histograms, showing the particle number distribution of some haematite sols having different modal diameters. The dark shaded distributions refer to sols being prepared by homogeneous nucleation. The light shaded histogram refers to a sample of Kerker et.al [48], prepared by heterogeneous nucleation.

2.4 RESULTS

2.4.1 Sols

(a) Sol synthesis: The seed sol appeared to be homodisperse as illustrated in figures 1 and 2. Applying the method of controlled nuclei growth under the conditions mentioned above we prepared homodisperse sols with particle radii up to 700 nm. Micrographs of some samples are shown in fig. 1. The dispersity of a number of sols is shown in fig. 2. The ratio between weight and number average particle radius never exceeded 1.03. Comparing the present results for the larger particle sizes with sols prepared by homogeneous nucleation proved that the former are much better homodisperse. To illustrate the difference, we included in fig. 2 a histogram of a sol prepared by homogeneous nucleation, described in ref. [48].

(b) Particle morphology: The shapes of the particles prepared by seeded growth proved to be drastically affected by changes in the concentrations of $FeCl_3$ and $HClO_4$ in solution as well as by the incubation time. An overview of some characteristic results, obtained for different combinations of $FeCl_3$ and $HClO_4$ concentrations at a fixed incubation time of 24 hours is shown in fig. 3. Nearly spherical particles resulted as a compromise of incubation

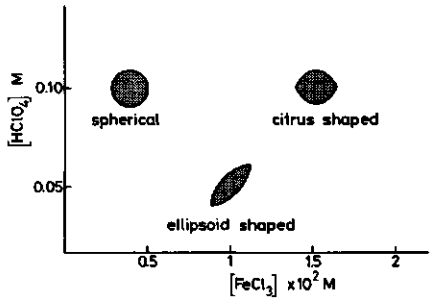

FIGURE 2.3. Schematic representation of the particle shapes obtained for different combinations of $FeCl_3$ and $HClO_4$ concentrations. Results relate to incubation times of 24 hours. Particles with spherical appearance in a satisfying yield were obtained only for restricted combinations of the concentrations of the two medium components. Incubation temperature: 100° C.

times of about 24 hours, low iron and intermediate acid concentrations. However, homodisperse particles with other shapes could be obtained by slightly altering the synthesis conditions (fig. 4).

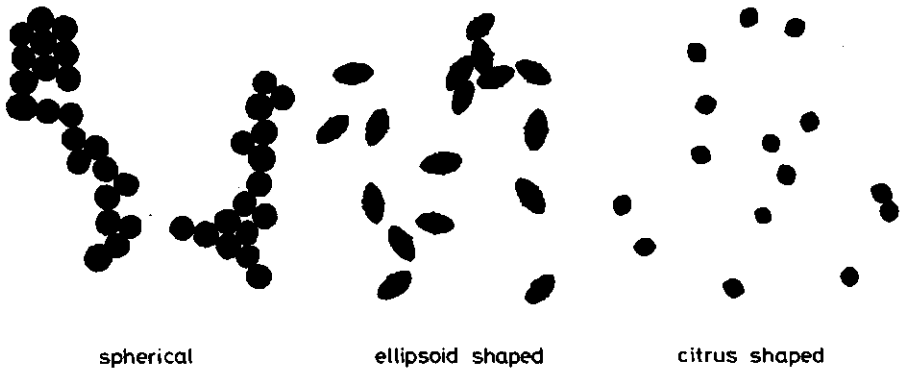

FIGURE 2.4. Some characteristic particle shapes observed under the electron microscope. For experimental conditions see fig. 2.3.

(c) Colour phenomena. The colour of the sols depended strongly on particle size, and changed from orange brown to dark purple with increasing diameter. When concentrated by evaporation, some of the sols (particle diameter 400-600 nm) exhibited clearly visible irridiscent colours. Stored in glass containers, sols with smaller particle size (diameter 200-400 nm) showed a metallic hue, probably due to particle accumulation on the container wall. The hue varied, depending on the particle size, from blue to red. Intermediate colours were also observed. The mentioned phenomena proved to be a criterion for homodispersity and uniformity of the samples, as they

were observed only for spherical and homodisperse sols.

(d) Crystal structure: The crystal structure of the particles was investigated by electron micro diffraction. Particles appeared to be monocrystalline, independent of their size and showed the crystallographic habit of α-Fe_2O_3 (haematite).

2.4.2 Growth kinetics

(a) Depletion experiments:

Unstirred suspensions: Some of the experiments, in which the decrease of free iron in solution was monitored as a function of time have been performed under non stirring conditions. Due to the high ionic strength of the solutions, the nuclei aggregated in an early stage of the precipitation process and sedimentated within one hour. Growth of the particles therefore occurred mainly in the sediment. Particle growth did not start immediately after the addition of the nuclei, but was delayed by a time t_i. However, after this induction time, which is strongly dependent on the concentration of $HClO_4$, the rate of condensation increased with increasing iron concentration, and to a first approximation it proved to be constant in time, as is shown in fig. 5. For $c > c_o$ the graph shows a proportionality up to about 0.018 M $FeCl_3$. Extrapolation of the line to zero growth rate gives an estimate of the solubility limit c_o. The slope of the linear part of the curve

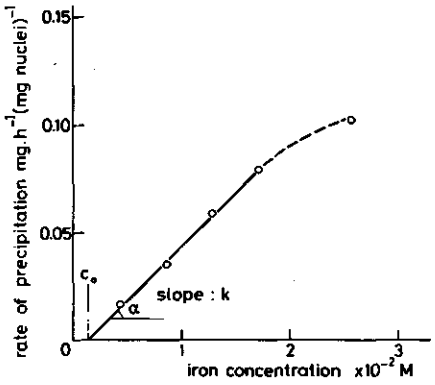

FIGURE 2.5. Dependence of the condensation rate on the iron concentration at 100°C in non-stirred solutions. The slope of the curve is related to the rate constant k_g. c_o is the saturation concentration of the solution.

is related to the growth rate k_g. As precipitation occurs in the sediment, i.e. the accessible surface on which growth can occur is determined by the contact plane between sediment and solution rather than by the surface of the individual particles, k_g will remain constant during the growth process,

and the weight increase can be expressed by the simple formula

$$dG/dt = k_g\ [c(t) - c_o] \qquad (2.2)$$

Using expression (2), and the derived values for k_g and c_o, we calculated for depletion experiments the increase in particle size as a function of time. A typical result is plotted in figure 6, together with experimental values. A good fit is obtained, assuming an induction period of 1.2 hours.

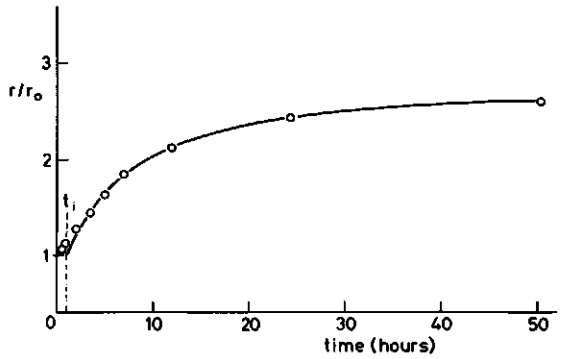

FIGURE 2.6. Increase in relative particle radius with time in non-stirred solutions at 100°C. The graph shows experimental values together with a calculated curve, using equation (2) and the kinetic parameters k and c_o, deduced from fig. 5. An induction time (t_1) of 1.2 hours has been assumed. The experiment was carried out in 5 ml volumes. The initial solution concentrations were 0.0134 M $FeCl_3$ and 0.15 M $HClO_4$. Reaction was started on t=0 by the addition of 0.263 mg of haematite nuclei (particle radius 45 nm).

Stirred suspensions: If the solution is stirred, the available surface area for precipitation, determined by the total particle surface area is not constant any more, but increases with time as the particles grow. Assuming diffusion controlled growth, kinetics should be governed by the equation [36]:

$$\frac{d[r(t)/r_o]^3}{dt} = 3\ D\ \frac{r(t)}{r_o}\ [c(t) - c_o]\ V\ r_o^{-2/3} \qquad (2.3)$$

In this formula r_o denotes the radius of the nuclei, r(t) the radius of the particles at time t, D the diffusion coefficient of the incorporated iron component, and V the molar volume of the solid phase, haematite [36]. These kinetics have indeed been found. In fig. 7, calculated and experimental data

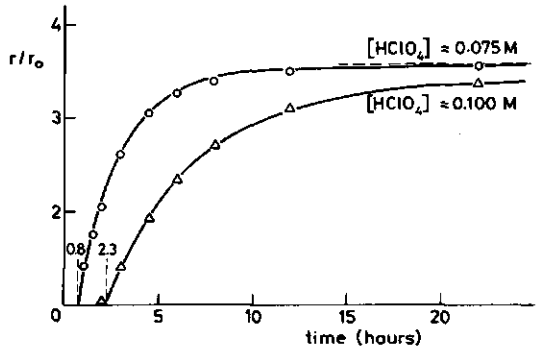

FIGURE 2.7. Relative increase of the particle radius with time in stirred suspensions at 100°C. The graph shows experimental values (O,Δ) and calculated curves (——) for two $HClO_4$ concentrations, assuming induction periods of 0.8 and 2.3 hours respectively. Reactions were started by adding 8.11 mg of haematite seed sol (particle radius 45 nm), to 450 ml solutions with an initial $FeCl_3$ concentration of 0.010 M.

on the relative increase of the particle radius with time are shown for two different perchloric acid concentrations.

The kinetics depend to a large extent on the acidity of the solution. A relatively small change in perchloric acid concentration has a considerable effect on the growth rate of the particles and on t_i. This is emphasized in fig. 8, in which the decrease of the iron concentration in solutions, containing variable amounts of $HClO_4$ is plotted as a function of the incubation time. At high acidity, the precipitation is preceded by partial dissolution of the particles, giving rise to a slight increase in the $FeCl_3$ concentration. The growth rate of the particles becomes very low if the $HClO_4$ concentration exceeds 0.19 M.

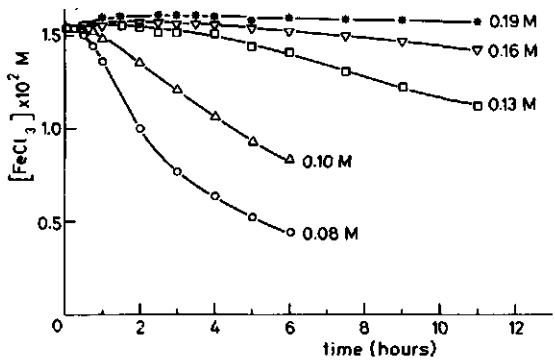

FIGURE 2.8. Decrease of the iron concentration with time in seeded, stirred suspensions at 100°C for different initial $HClO_4$ concentrations (indicated). Reactions were started by adding 4.11 mg haematite nuclei (particle radius 45 nm), to 80 ml of solution.

(b) Precipitation at constant supersaturation: Equation (3) can be modified, yielding

$$\frac{d[r(t)]^2}{dt} = 2\ D\ [c(t) - c_o]\ V \qquad (2.4)$$

In diffusion controlled processes therefore the increase of the surface area of spherical particles with time should be constant, provided the supersaturation is kept at its initial value. In fig. 9, the relative increase of the surface area due to particle growth at constant supersaturation is given for solutions, having the same iron concentration, but which differ with respect to the $HClO_4$ content. All curves are linear, indicating that diffusion-control persists over the entire concentration range studied. The

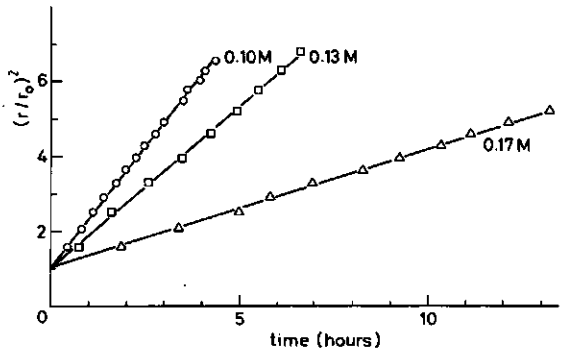

FIGURE 2.9. Increase of the relative particle surface area with time at fixed supersaturation for different concentrations of $HClO_4$. Iron concentration in all cases: 0.015 M, temperature: 100°C. Initiation: see fig. 2.8.

lines start at unit relative surface area. In these experiments no induction times are observed, i.e. the nuclei start to grow immediately after addition of nuclei to the incubation medium. It should be mentioned however, that in other experiments we observed induction times of up to two hours. This difference might be attributed to inadvertent contamination with traces of impurities. (The influence of contaminants on the onset of precipitation reactions has been pointed out before [39]). Within sets of comparable experiments, the logarithm of the induction time showed a linear dependence on solution acidity as is examplified in fig. 10.

The influence of the temperature on the growth rate is shown in fig. 11. A decrease of the incubation temperature from 100°C to 97°C reduces the particle growth rate by a factor of about two. Increase of the temperature back to 100°C restores the original growth rate.

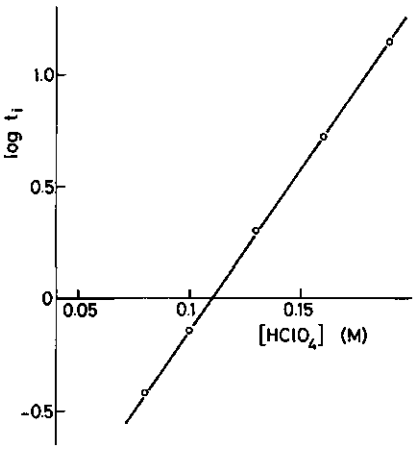

FIGURE 2.10. Logarithm of the incubation time t_i as a function of the perchloric acid concentration in solution. Iron concentration: 0.015 M, temperature : 100°C. Initiation : see fig. 8.

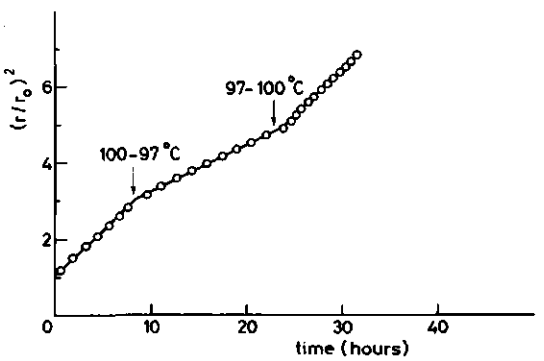

FIGURE 2.11. Influence of temperature-changes on the rate of condensation in seeded solutions, kept at constant supersaturation (0.01 M $FeCl_3$ and 0.155 M $HClO_4$). Initiation : see fig. 8. At the time, indicated by arrow 1, the temperature is decreased to 97°C. The initial temperature of 100°C is restored at the time indicated by arrow 2.

2.5 DISCUSSION

In recent years, considerable effort has been made in unraveling the mechanism of homogeneous nucleation and growth of iron (hydrous) oxides, and evidence accumulated of the complexity of the process, which involves hydrolysis, complex formation, polymerisation and aggregation [40-43]. As a consequence, any experimental attempt to monitor the condensation of colloidal oxides from homogeneous solutions proves to be arduous. However, by choosing conditions under which any spontaneous nucleation during the time scale of the experiments is suppressed, so that only growth of known amounts of seed crystals is allowed, the condensation process becomes better amenable to

kinetic measurements and hence to control. In the experiments described, homogeneous nucleation was avoided by lowering the pH of the iron(III) chloride solutions used. In such a way, formation of polymeric iron species, (the precursors of oxide formation), and hence the spontaneous generation of a new solid phase was prevented.

Depletion experiments, as well as experiments carried out at constant supersaturation indicate that under the conditions chosen, particle growth is diffusion-controlled. Both kinetic approaches enable the computation of the diffusion coefficient of the species being incorporated in the solid phase [36]. The values of D, obtained from the two kinds of experiments agree very well mutually, the difference being less than 10%. However, the apparent coefficients are rather large, and tend to decrease with increasing perchloric acid concentration from 3.9×10^{-4} cm^2/sec in 0.075 M $HClO_4$ to $3.3 \times 10^{-5} cm^2/sec$ in 0.017 M $HClO_4$. This trend might be attributed to acid-induced equilibria shifts from free Fe^{3+} to small iron-hydroxy and iron-chloride complexes, some of which are considered to play an active part in the condensation process. The importance of such shifts has been pointed out before: based on experimentally determined equilibrium constants, Sapieszko et. al. [45] calculated the distribution of iron over the hydroxy complexes involved. At high temperatures and low acidity, the formation of $Fe(OH)_2^+$, $Fe(OH)^{2+}$, and $Fe_2(OH)_2^{4+}$ appears to be considerably enhanced by only a slight increase in pH value. In our case a full quantitative kinetic interpretation can not be given, partly because of the complexity of the system (a.o. the role of Cl^- is difficult to assess), partly because of lack of equilibrium data at elevated temperatures. Yet, equilibria shifts qualitatively account for the differences in the rate of condensation at different acid concentrations.

The mentioned diffusion coefficients have no simple physical meaning as they cannot be assigned unambiguously to one specific iron complex. Their magnitudes however, exceeding that of hydrated simple ions indicate that the condensation rate is not purely diffusion controlled, but enhanced by convection. That convection may not be neglected, even though the particles in situ are small and growth occured at moderate stirring rates, is due to aggregate formation in the growth medium in which the ionic strength is far above the coagulation value of the haematite nuclei. As it is the aggregate size rather than the individual particle size which determines convection, its contribution will not change during the growth process as long as the

hydrodynamic conditions (i.e. stirring rate) in the reaction vessel are not altered.

In this context it should be stressed that despite aggregate formation, regular and homodisperse particles are obtained. This result is quite unexpected, as diffusional growth in particle agglomerates will allways give rise to irregular, differently sized particles, because of different positions inside the agglomerate. We therefore believe that the flocculation is reversible under the applied experimental conditions, i.e. the time scales of aggregation and subsequent repeptisation are similar and small compared with the time scale of growth.

A matter of particular interest is the appearance of the induction time t_i which was observed in some condensation reactions. In sets of comparable experiments, performed at different acidity, t_i shows a logarithmic dependence on acid concentration, suggesting that particle growth is initiated by the formation of critical surface nuclei. The free energy of nuclei generation, and hence the length of the induction time is influenced by the presence of traces of anionic impurities. This experience is substantiated by our experience that the induction times could differ sometimes by as much as a factor of 10 between solutions prepared from different batches of $FeCl_3$. In addition, the shape of the precipitated phase differed as a possible consequence of impurity adsorption on the nuclei [36, 37]. Subsequent investigations showed that this behaviour is due to the presence of phosphate. Phosphate ions, of which the special adsorption properties on haematite have been noted before [47], added to the reaction fluid in amounts which are within the impurity specifications of p.a. $FeCl_3$ supplied by some manufacturers, had a considerable effect on the morphology of the precipitated phase. This emphasizes the high purity requirements for chemicals and glassware used throughout the experiments. To obtain consistent results, $FeCl_3$ with a phosphate ion concentration smaller then 5 ppm should be used.

The presence of small amounts of chloride proved to be essential for the synthesis of homodisperse, spherically shaped particles. However, no growth at all appeared, if instead of perchloric acid, hydrochloric acid was used to attain high acidity, emphasizing the role of the chloride ion in the complex formation. In addition to the nature of the anion, factors like the rate of condensation, the iron concentration and acid content influence the particle shape to a large extent. Establishing conditions which give rise to the formation of nearly spherical particles, suiting our demands, therefore

appeared to be an arduous job. However, once set, the preparation of spherically shaped particles could be carried out without great difficulties and with high reproducibility.

In following reports we intend to deal with the optical and electrochemical characterisation of the sols.

2.6 CONCLUSIONS

In this report, a method is described for the synthesis of homodisperse haematite (α-Fe_2O_3) sols, consisting of particles whose radii can be adjusted from about 40 nm up to almost micron size. The method is based on the principle of seeded growth. In practice it is carried out by adding haematite seeds to a heated (and therefore supersaturated) acidified solution of $FeCl_3$. It was the aim of the study to develop a procedure for the preparation of spherically shaped particles. However, only slight alterations of the synthesis conditions were needed to cause formation of other paricle shapes. The end products proved to be monocrystalline and for present standards highly homodisperse. The latter is emphasized by the characteristic optical behaviour of the purified sols.

Kinetic experiments, performed to unravel the underlying mechanisms of particle growth showed that the precipitation of oxide on the seeds from the supersaturated $FeCl_3$ solutions is governed by diffusion. The presence of Cl^- proved to be essential for the synthesis of spherical particles, but no chloride could be detected in the core material of the particles finally being formed.

Because of their morphological features, their indifference regarding rigorous treatment such as ultrasonication, high stability and the apparent absence of aging effects, the sols obtained are suitable model systems for colloid chemical studies.

2.7 ACKNOWLEDGEMENTS

We wish to thank Mr. H. G. Elerie and Mr. A. Boekestein of the TFDL for their kind assistance with the electron microscope and its application in microdiffraction. We also acknowledge Mr. Schoonderbeek of the STIBOKA for

carrying out the particle sizing, and professor L. van der Plas for his guidance in the interpretation of the diffraction results.

2.8 REFERENCES

(1) Goodwin, H.M., Z. Phys. Chem. **21**, 1 (1896).

(2) Pean de St. Gilles, Compt. Rend. **40**, 568 (1855).

(3) Graham, T., J. Chem. Soc. 15, 250 (1862).

(4) Parks, G.A., Chem. Rev. **65**, 177 (1965).

(5) Sylva R.N., Rev. Pure Appl. Chem. **22**, 115 (1972).

(6) Kennedy J.T., Townsend, W.P., and Emerson, J.A., J. Colloid Interface Sci. **42**, 589 (1973).

(7) Wolf, R.H.H., Wrischer, M., and Sipalo-Zuljević, Kolloid-Z. Z. Polym. **215**, 57 (1967).

(8) Atkinson, R.J., Posner, A.M., and Quirk, J.P., J. Inorg. Nucl. Chem. **30**, 2371 (1968).

(9) Spiro, T.G., Pape, L., and Saltman, P., J. Amer. Chem. Soc. **89**, 5555 (1967).

(10) Watson, J.H.L., Cardell, R.R., Jr., and Heller W., J. Phys. Chem. **66**, 1757 (1962).

(11) Spiro, T.G., Allerton, S.E., Renner, J., Terzis, A., Bills, R., and Saltman, P., J. Amer. Chem. Soc. **88**, 2721 (1966).

(12) Steele, F.A., J. Colloid Sci. **9**, 166 (1954).

(13) Matijević, E., Lindsay, A.D., Kratohvil, S., Jones, M.E., and Larson, R.L., J. Colloid Interface Sci. **36**, 273 (1971).

(14) Demchack, R., and Matijević, E., J. Inorg. Nucl. Chem. **35**, 3691 (1973).

(15) Brace, R., and Matijević, E., J. Inorg. Nucl. Chem. **35**, 3691 (1973).

(16) Catone, D.L., and Matijević, E., J. Colloid Interface Sci. **48**, 291 (1974).

(17) Mc. Fayden, P., and Matijević, E., J. Colloid Interface Sci. **44**, 95 (1973).

(18) Matijević, E., Accounts Chem. Res. **14**, 22 (1981).

(19) Matijević, E., Pure Appl. Chem. **50**, 1193 (1978).

(20) Matijević, E., Progr. Colloid Polym. Sci. **61**, 24 (1976).

(21) Matijević, E., and Scheiner, P., J. Colloid Interface Sci. **63**, 509 (1978).

(22) Sugimoto, T., and Matijević, E., J. Colloid Interface Sci. **74**, 227 (1980).

(23) Matijević, E., Sapieszko, R.S., Melville, J.B., J. Colloid Interface Sci. **50**, 567 (1975).

(24) Hamada, S., Matijević, E., J. Colloid Interface Sci. **84**, 274 (1981).

(25) Joekes, I., Galembeck, F., Souza-Santos, H., Jafelicci, M., J. Colloid Interface Sci. **84**, 278 (1981).

(26) Davies, C.W., and Jones, A.L., Trans. Faraday Soc. **51**, 812 (1955).

(27) Howard, J.R. and Nancollas, G.H., Trans. Faraday Soc. **53**, 1449 (1957).

(28) Nancollas, G.H., and Purdic, N., Quart. Rev. London **18**, 1 (1964).

(29) Davies, C.W., and Jones, A.L., Faraday Soc. Discuss. **5**, 111 (1949).

(30) Nancollas, G.H., Reddy, M.M., and Tsai, F., J. Cryst. Growth **20**, 125 (1973).

(31) Gardener, G.L., and Nancollas, G.H., J. Cryst. Growth **21**, 267 (1974).

(32) Liu, S.T., and Nancollas, G.H., J. Cryst. Growth **6**, 281 (1970).

(33) Liu, S.T., and Nancollas, G.H., Pet. Eng. J. **509** (1975).

(34) Walton, A.G.,; "The formation and Properties of Precipitates". Chem. Anal., Vol. 23 (Elving, P.J., and Kolthoff, I.M., ed.) Intersci. Publ. John Wiley and Sons, New York, London, Sidney (1967).

(35) Matijević, E., and Wilhelmy, D.M., J. Colloid Interface Sci. **86**, 476 (1982).

(36) Nielsen, A.E., "Kinetics of Precipitation". Pergamon Press, Oxford (1964).

(37) Vogel, A.I., "A Textbook of Quantitative Inorganic Analysis", 3 ed. Longmans, Green and Co. Ltd., London, 786 (1961).

(38) Ives, D.J.G., and Janz, G.J., "Reference Electrodes. Theory and Practice". Academic Press, p. 179 (1961).

(39) Nielsen, A.E., "Kinetics of Precipitation". Pergamon, Oxford, p.120 (1964).

(40) Douwsma, J., "A Colloidal Chemical Study of the Formation of Iron Oxyhydroxide". Thesis,Utrecht (1979).

(41) Douwsma, J., and de Bruyn, P.L., J. Colloid Interface Sci. **56**, 527 (1976).

(42) Douwsma, J., and De Bruyn, P.L., J. Colloid Interface Sci. **64**, 154 (1978).

(43) Musić, S., Vertes, A., Simmons, G.W., Czako-Nagy, I., Leidheiser Jr., H., J. Colloid Interface Sci. **85**, 256 (1982).

(44) Eisenlauer, J., and Matijević, E., J. Colloid Interface Sci. **75**, 199 (1980).

(45) Sapieszko, R.S., Patel, R.C., Matijević, E., J. Phys. Chem. **81**, 1061 (1977).

(46) Buckley, H.E., "Crystal Growth". Wiley, New York (1951).

(47) Breeuwsma, A., "Adsorption of Ions on Hematite (α-Fe_2O_3)".Ph.D. thesis, Agricultural University Wageningen (Neth.) (1973).

(48) Kerker, M., Scheiner P., Cooke, D.D., and Kratohvil, J.P., J. Colloid Interface Sci. **71**, 1979.

III. TURBIDITY OF HOMODISPERSE HAEMATITE (α-Fe_2O_3) HYDROSOLS

3.1 ABSTRACT

Turbidity measurements, carried out at wavelengths from 400 to 800 nm on homodisperse haematite (α-Fe_2O_3) hydrosols with particle diameters ranging from 30 to 500 nm are compared with calculations based upon Mie's scattering theory for homogeneous isotropic spheres. The agreement between experimental and calculated values is good for any particle size and wavelength, despite the monocrystalline nature of the scatterer and the resulting deviation from sphericity. The experiments support the dependence of the absorption coefficient on wavelength as proposed by Kerker [20,21].

3.2 INTRODUCTION

Because of the ubiquity of light scattering phenomena in nature, there has been an early interest of science in theories which relate the properties of the scatterer (i.e. its size, shape, absorption coefficient and real part of the refractive index) to the scattering behaviour. For homgeneous, isotropic, spherical particles of arbitrary size and material, general theoretical relations, now known as the Mie theory [1-4], were developed.

For colloid systems the agreement between theory and experiment has been explored extensively, using a variety of homodisperse hydrosols, some of them consisting of dielectric spheres (latex [5-9], sulphur [10,11], silica [13,14]), others exhibiting absorption (sulphur in the IR region [12], gold [15], selenium [16,17]). Ever since, the practical application of light scattering has assumed extended proportions, and a comprehensive review of scattering experiments, performed to characterize colloidal systems with regard to size distribution and optical constants could hardly be exhaustive.

Of the optical constants, the absorption coefficient κ is an important, though elusive, parameter. For highly absorbing media it dominates the colour, thus playing a crucial role in the optical characteristics of pigments [18,19]. A pigment of considerable commercial importance is haematite (α-Fe_2O_3). Its optical properties have been elucidated, using turbidity and scattering data of hydrosols, containing α-Fe_2O_3 particles, small enough to

be treated as Rayleigh scatterers [20,21].

Recently we succeeded in developing a method for the preparation of haematite hydrosols, containing homodisperse, approximately spherical particles within a large range of particle sizes exceeding the Rayleigh region [22]. These sols are useful model systems for scattering analysis.

This report describes the comparison between measured and calculated turbidities with the aim to explore the optical properties of colloidal haematite and to extend Kerkers [20] experiments.

3.3 EXPERIMENTAL

3.3.1 Haematite sols

The haematite hydrosols were prepared according to a procedure, outlined in a previous paper [22] (see chapter 2). The diameters of the particles in the test systems ranged from 30 up to 500 nm, thus covering a large spectrum of α-values where $\alpha = 2 \pi n r/\lambda$, n being the real part of the refractive index, r the particle radius and λ the wavelength in vacuum of the light used.

3.3.2 Concentration

The haematite content in the hydrosols was determined by dissolving known amounts of sol in concentrated hydrochloric acid. After dilution, the iron concentration was analyzed, using a modified thiocyanate method [22].

3.3.3 Turbidity measurements

Turbidities were measured using a Varian model DMS 80 spectrophotometer. In order to reduce the amount of low angle scattering, the apparatus was adapted with diaphragms, limiting the angle of acceptance of the photo cell to 2.5 degrees. All turbidity measurements have been performed in 10^{-3} M $HClO_4$ to prevent coagulation. Possible aggregate formation was reduced by subjecting all samples to ultrasonication prior to the measurements. The concentration of suspended haematite was adjusted to the particle size and varied from 114 microgram/ml up to 557 microgram/ml. In this range, measurements could be carried out without interference of multiple scattering.

3.3.4 Optical constants

The calculations presented in this report are based upon values of the

refractive index and absorption coefficient proposed by Kerker [20]. They describe the optical behaviour of our systems satisfactorily. Relative index values have been comprised in Fig.1. The existing scattering theories apply to isotropic spheres. However, the sols consist of monocrystalline [22] uniaxial particles. Therefore the indices are averages, weighting the ordinary (n_ω) and extraordinary (n_ε) rays in a ratio 2 to 1 [20,21,23].

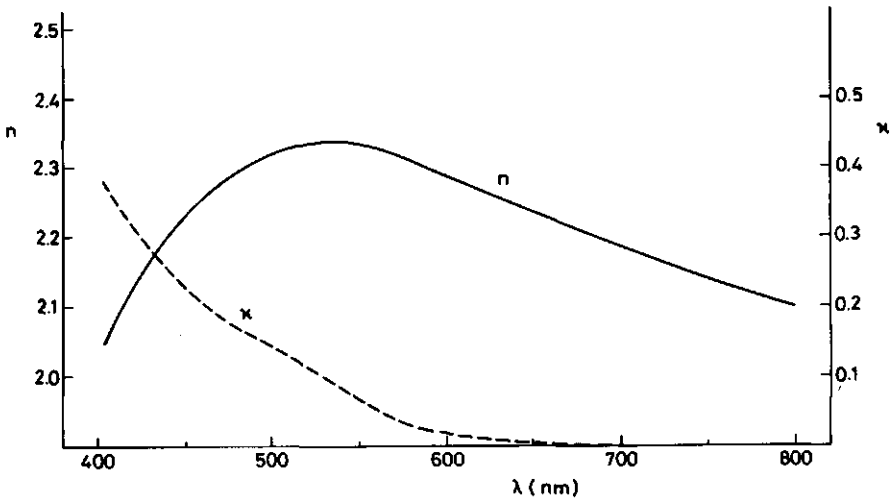

FIGURE 3.1. Real part of the refractive index n, and its imaginary part (absorption coefficient κ) versus wavelength. Plots were obtained from ref. [20] and [21].

3.3.5 Particle size and shape

Size distributions were measured with the aid of a Philips 400 T electron microscope. Accurate data could be obtained by photographing sample grids as well as a standard diffraction grating of 21600 lines/cm at the same focal plane and magnification. Electron micrographs were then sized on a Quantimet 720 assuming that the projected particle area can be approximated by the projection area of a sphere. Average particle radii, obtained in this way will be referred to as r_{EM}. The sols proved to be extremely homodisperse; the ratio between weight and number average particle size never exceeded 1.03 [22]. For some sol samples, the particle size has been verified by measuring the rate of sedimentation. Hydrodynamic radii were significantly smaller. This is due to the fact that the particles are no perfect spheres (see section results and discussion).

Scanning electron micrographs have been performed with the aid of a Jeol 35 C microscope equipped with a lanthanum hexabromide gun to enhance resolution. Samples were deposited on gold-coated glass carriers and subsequently coated with an additional gold film to avoid charging.

3.3.6 Calculations

Calculations have been carried out on a Digital Equipment Corporation DEC 10 computer system. Programmes were written in SIMULA, using algorithms based on Mie scattering theory as outlined in ref. [4].

3.4 RESULTS AND DISCUSSION

In the initial stage of the investigation we tried to relate measured specific turbidities for several averaged projected area radii (r_{EM}) to calculated values, using the optical constants as proposed by Kerker [20]. The agreement between calculated and measured values was poor, indicating either wrong values for the absorption coefficient (κ), the refractive index (η), or the occurence of a critical dependence of the optical properties on the distribution width. Any attempt to achieve improvement by refining existing computer programmes failed: neither taking into account the actual size distribution, nor the optimalisation of n and κ, applying an iterative procedure, gave rise to good results. Therefore, the particle size was considered to be incorrect, and calculations were performed with Kerker's values for n and κ. In this case, a satisfactory agreement was attained for any wavelength in the visible range, assuming averaged particle radii of 0.8 times r_{EM}. (This corrected particle size will be referred to as r_{LS}.) Results are shown in fig. 2, where calculated turbidity spectra in the visible range are related to experimental curves for different scattering radii.

The theoretical dependencies of the specific turbidity on particle size for strictly homodisperse Fe_2O_3 sols containing spherical particles are shown in fig. 3-5 for three different wavelengths. The curves exhibit a pronounced ripple structure at higher wavelengths, a well known feature for highly refractive particles exhibiting only little absorption [3-4]. At 400 nm, ripples are absent due to the considerable contribution of absorption. Experimental values are incorporated in the figures, giving evidence of a good agreement over the whole wavelength range.

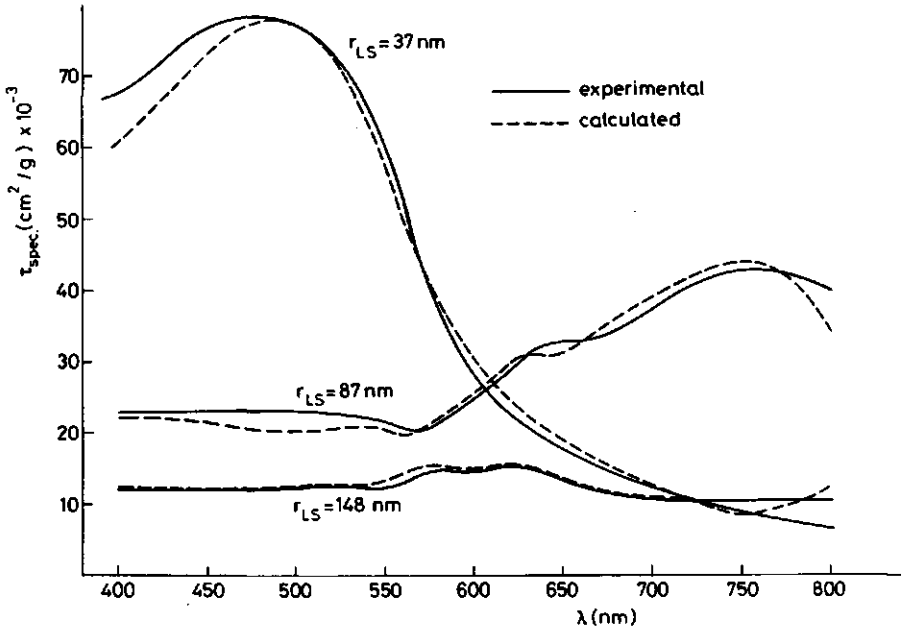

FIGURE 3.2. Calculated (----) and experimental (——) turbidity spectra for three different average particle sizes. The average scattering radius (r_{LS}) is assumed to be 0.8 times the average projected area radius (r_{EM}). In the calculations, the actual size distribution of the sols has been taken into account.

Determination of the hydrodynamic radii by means of sedimentation experiments, performed for bigger particles resulted in particle sizes in close agreement to scattering results, indicating that the difference between projected- and scattering radii must be accounted for by shape effects. As reported earlier [22] (chapter 2), the haematite particles used throughout the investigations are monocrystalline. Their transmission electron micrographs (two dimensional projections) suggest a more or less spherical shape, but they might not reflect the actual crystalline morphology. More information about particle shape is obtained from scanning electron micrographs (figure 6), giving insight in the surface structure. Particles appear to be rounded, cubically shaped, with some variety with respect to crystal morphology. The projected area of such particles will overestimate the size when interpreted as the two dimensional projection of a sphere. However, because of the uniformity in shape between particles of different average dimensions, the correction which has to be applied to account for the deviation from sphericity is independent of particle size.

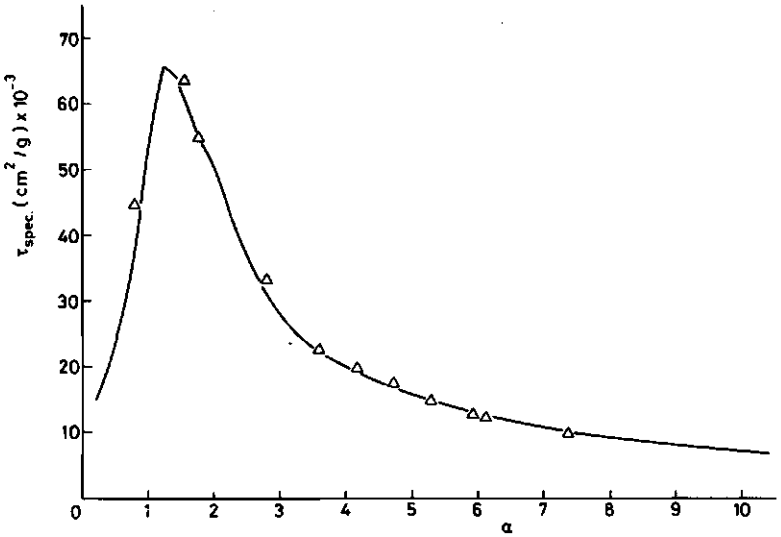

FIGURE 3.3. Experimental (Δ) and calculated (——) specific turbidity versus size parameter. Wavelength: 400 nm. Interval width between calculated data points: 10 nm.

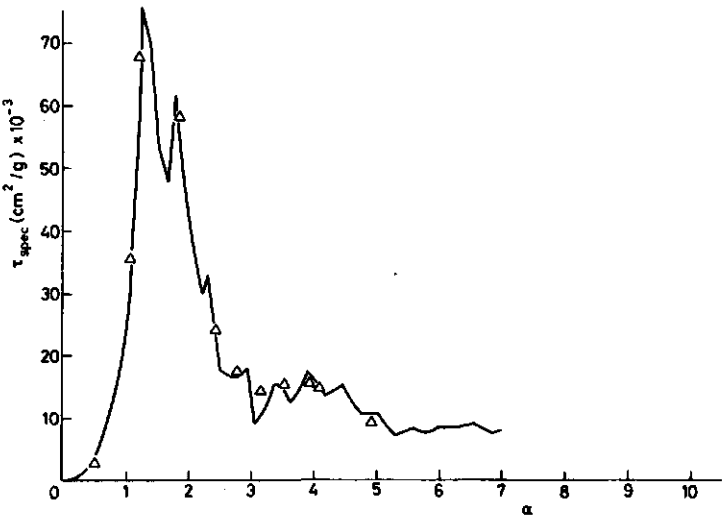

FIGURE 3.4. Experimental (Δ) and calculated (——) specific turbidity versus size parameter. Wavelength: 600 nm. Interval width between calculated data points: 10 nm.

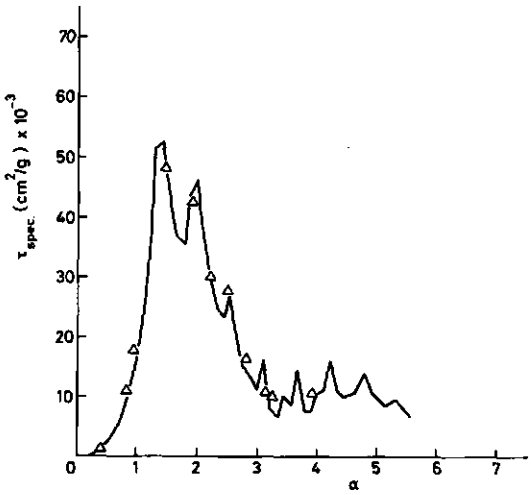

FIGURE 3.5. Experimental (Δ) and calculated (——) specific turbidity versus size parameter. Wavelength: 750 nm. Interval width between calculated data points: 10 nm.

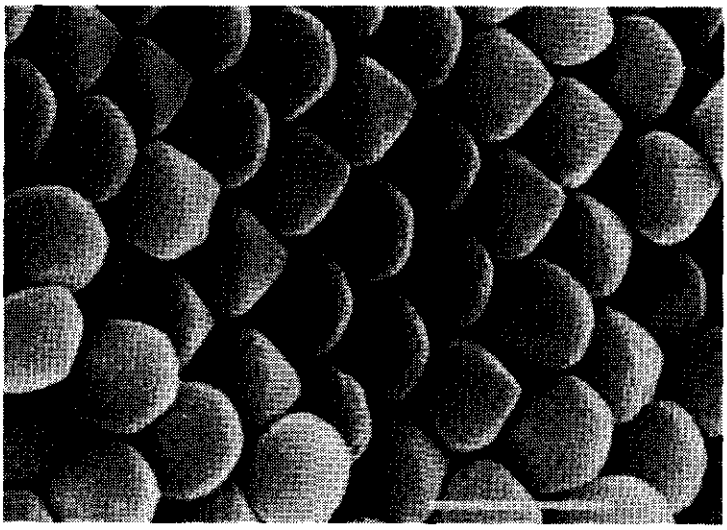

FIGURE 3.6. Scanning electron micrograph of a haematite sol sample (r_{LS}=292 nm). The bar refers to 1 μm.

At present, there is no general theory for the calculation of the light scattering of non-spherical particles of arbitrary size and any combination of real refractive and absorption index. The development of rigorous analytical methods is still in an embryonal stage [24], and present approaches are restricted in their applicability because they either assume the particles to be non-absorbing, or restrict their analysis to ellipsoid particles

in the Rayleigh-Debye domain [25-28]. In this context is should be pointed out, that despite considerable deviations from sphericity, the investigated monocrystalline haematite scatterers can be adequately described with the Mie theory for homogeneous isotropic spheres, irrespective of particle size.

However unexpected this result might be, it may justify the use of such scattering calculations in the description of the colour of iron oxide pigments.

For our aims, the agreement between theory and experiments provides the fundament for the quantitative interpretation of turbidity changes in coagulating systems. A next report will deal with this problem.

3.5 CONCLUSIONS

The homodisperse haematite sols, whose synthesis has been described before [22], proved to be suited model systems for the investigation of the optical properties of the iron oxide. The refractive index (n) and the absorption coefficient (κ) for α-Fe_2O_3 could be determined by the comparsion of experimental turbidity data, obtained for different wavelengths and particle sizes, with calculated values based upon the Mie scattering theory for isotropic spheres.

The agreement between experimental and calculated values is good, even though the particles under study are monocrystalline (and therefore optically anisotropic), and show profound deviations from sphericity.

3.6 ACKNOWLEDGEMENTS

We wish to thank Mr. F. Thiel for the skilled performing of the scanning experiments, and Ir. J. Scheutjens and Ir. J. Papenhuijzen for their patient aid in designing the programmes.

3.7 REFERENCES

(1) Mie, G., Ann. Phys. (Leibzig) **25**, 377 (1908).

(2) Debye, P., Ann. Phys. (Leibzig) **30**, 57 (1909).

(3) van de Hulst, H.C., "Light Scattering by Small Particles." Wiley, New York (1957).

(4) Kerker, M., "The Scattering of Light and other Electromagnetic Radiation." Academic Press, New York (1969).

(5) Kratohvil, J.P., and Smart, C., J. Colloid Sci. **20**, 875 (1965).

(6) Deželić, G., and Kratohvil, J.P., J. Colloid Sci. **16**, 561 (1961).

(7) Bateman, J.B., Weneck, E.J., and Eshler, D.C., J. Colloid Sci. **14**, 308 (1959).

(8) Tabibian, R.M., Heller, W., and Epel J.N., J. Colloid Sci. **11**, 195 (1956).

(9) Aron, S.H., Pierce, P.E., J. Polym. Sci., Polym. Chem. Ed. **27**, 183 (1969)

(10) Barnes, M.D., and La Mer, V.K., J. Colloid Sci. **1**, 79 (1946).

(11) Barnes, M.D., Kenyon, A.S., Zaiser, E.M., and La Mer, V.K., J. Colloid Sci. **2**, 349 (1947).

(12) Kenyon, A.S., and La Mer, V.K., J. Colloid Sci. **4**, 163 (1949).

(13) Deželić, G., and Kratohvil, J.P., Kolloid-Z Z. Polym. **173**, 38 (1960).

(14) Kratohvil, J.P., and Deželić, G., Kolloid-Z. Z. Polym. **180**, 67 (1962).

(15) Turkevich, J., Garton, G., and Stevenson, P.C., J. Colloid Sci. Suppl. 1, 26 (1954).

(16) Dauchot, J., and Watillon, A., J. Colloid Interface Sci. **23**, 62 (1967).

(17) Watillon, A., and Dauchot, J., J. Colloid Interface Sci. **27**(3), 507 (1968).

(18) Chromey, F.C., J. Opt. Soc. Amer. **50**, 730 (1960).

(19) Volz, H.G., Angew. Chem., Int. Edit. **14**, 688 (1975).

(20) Kerker, M., Scheiner, P., Cooke, D.D., and Kratohvil, J.P., J. Colloid Interface Sci. **71** (1), 176 (1979).

(21) Scheiner, P., "Preparation and Optical Properties of Colloidal Ferric Hydrous Oxides." Ph.D. Thesis, Clarkson College of Technology, Potsdam, N.Y. (1979).

(22) Penners, N.H.G. and L.K. Koopal, Colloids and Surfaces, submitted.

(23) Larsen, E.S., U.S. Geol. Survey Bull. 679 (1921).

(24) Barber, P.W., and Massoudi. H., Aerosol Science and Technology **1**, 303 (1982).

(25) Latimer, P., J. Colloid Interface Sci. **53**, 102 (1975).

(26) Nakagaki, M., J. Phys. Chem. **84**, 1587 (1980).

(27) Napper, D.H., Kolloid-Z. Z. Polym. **223** (2), 141 (1967).

(28) Petres, J.J. Deželić G., J. Colloid Interface Sci. **50** (2) 297 (1975).

IV. INTERFACIAL ELECTROCHEMISTRY OF HAEMATITE

4.1 ABSTRACT

Potentiometric titrations and electrophoretic mobility studies of aqueous sols as well as streaming potential measurements on haematite-coated glass capillaries have been used to characterise the surface properties of different kinds of haematite (α-Fe_2O_3). Depending on their origin and pretreatment, the samples exhibit a different equilibration and charging behaviour. The location of the point of zero charge however is insensitive to the origin of the oxide whereas ionic contaminants cause substantial shifts. The observed charge differences between different samples have been attributed to pH-dependent surface modifications involving amorphous iron(hydr)oxides.

Due to dehydration of the surface, the point of zero charge decreases by about 3 pH units if the haematite is dried or heated. In contradiction to the non heated oxide, the heated material shows a specific affinity for chloride.

Electrophoretic mobility studies are in good agreement with the titration results. Both indicate a point of zero charge value of about 9.5 for the untreated hydrosols.

4.2 INTRODUCTION

Several polymorphic forms of iron oxides constitute the end product of corrosion processes involving iron and iron alloys. Because of the economic relevance of these processes a considerable amount of work has been devoted to unravel the complex mechanisms of the formation and the final properties of the colloidal iron compounds formed [1-5]. With regard to the latter, the electrochemical characteristics are of outmost importance as they govern the adsorptive capacity for ions, stability, and adhesion behaviour. Such factors are the source of many problems which have to be faced in practice, for example in maintaining the cooling circuits of nuclear power plants [4,6].

One of the crystallographic modifications of the iron oxide is haematite (α-Fe_2O_3). Its electrochemical behaviour has been studied extensively [5,7,8], using mainly potentiometric acid-base titrations and microelectro-

phoresis as the experimental tools. Together with work done on other oxides [7], it established our understanding in the charging mechanisms of oxide surfaces. Theories have been developed which relate the pristine point of zero charge (p.p.z.c, a formulation adapted in analogy with the nomenclature used by Lyklema [9]) of the oxide materials to the valence of the metal cation, its coordination, and crystallographic dimensions [7,10]. Despite their relative simple nature these theories predict experimental results satisfactorily for many oxides over a whole range of accessible pH values.

However, even though the major lines of behaviour of oxides might be well established, there are a number of electrochemical aspects which deserve further exploration: one of them is that oxides have shown to develop high surface charge densities compared with other substrates [11]. A porous surface structure, probably originated in pH-induced changes in the morphological habit of the surface has been proposed to account for this fact [5,7,11,12]. Such a diffuse surface structure will have direct consequences for the validity of charging models which have been developed to calculate the surface charge density σ_0 as a function of medium conditions (pH, electrolyte concentration), assuming hard and nonporous surfaces [13,14]. Another matter of interest is the dependence of the electrochemical properties of the oxides on pretreatment as observed for RuO_2 [15], TiO_2 [16,17], Fe_3O_4 [18] and α-Fe_2O_3 [17]. "History effects" indicate that not only basic crystallographic characteristics govern the electrochemical properties of oxides. Also changes in surface stoichiometry might be of major importance.

It is the aim of this paper to contribute to the mentioned discussion points by showing that haematite colloids, that are identical from a crystallographic point of view, exhibit different electrochemical surface properties. In this report, monodisperse samples of the "forced hydrolysis" type, obtained by precipitation from acidified solutions at elevated temperatures [19] (see chapter 2) are compared with "Breeuwsma" autoclaved haematite, produced by alkaline precipitation at room temperature [5]. These two samples are representative for two major procedures applied in haematite synthesis under laboratory conditions. The comparsion is mainly based on potentiometric titrations, electrophoresis and streaming potential measurements.

4.3 EXPERIMENTAL

4.3.1 Hydrosols

Sample (a), homodisperse haematite: The homodisperse haematite hydrosols used throughout most of the experiments were prepared by hydrolysis of acidified $FeCl_3$ solutions, following a procedure outlined in a previous paper [19] (see also chapter 2). Because the small size samples had the most favourable area/volume ratio, the titration experiments were carried out with hydrosols containing small particles (radius ≈ 40 nm).

Sample (b), Breeuwsma haematite: Since 1970, a considerable amount of experimental work, concerning the adsorption of ions [5,20] and proteins [21], has been compiled on haematite prepared by Breeuwsma [5]. In order to enable comparsion, we included one of Breeuwsma's original samples in the experiments. It contained irregularly shaped, heterodisperse particles with radii of about 50 nm.

Sample (c), coated-Breeuwsma haematite: Breeuwsma haematite particles were covered with a thin layer of haematite under conditions maintained in the production of the homodisperse samples (a): The sol was immersed in a supersaturated acidified solution of $FeCl_3$, in analogy with the procedure outlined in [19] (chapter 2). The haematite particles behave like seeds and initiate surface precipitation. The weight ratio between potential precipitate and total weight of the particles after coating was chosen to be 0.3. Under such circumstances, a thin surface layer will develop without changing the particle shape and size significantly, at least if the precipitate is deposited homogeneously over the particle surface. Hence, the surface properties of sample (c) and (a) should be identical.

Sample (d), ignited Breeuwsma haematite: In order to gain insight in the influence of temperature treatment on the properties of the oxide, part of the Breeuwsma haemtite was freeze-dried and subsequently heated to 560° C for about 6 hours.

4.3.2 Specific surface area

The specific surface areas of the haematites were obtained from BET N_2 adsorption on freeze-dried samples. The values for the homodisperse haematite (a), Breeuwsma's sample (b) and the coated oxide (c) are 26.5, 29.6, and 27.4 m^2/g. The specific surface area for the heat treated sample (d) however was considerably lower with 13 m^2/g, indicating sintering of the

oxide particles. The slight difference in specific surface area between (b) and (c) indicates that indeed a homogeneously spread layer has been formed during the coating process.

4.3.3 Surface charge measurements

Titrations were carried out at 21° C in aqueous suspensions of Fe_2O_3 with KCl as the supporting electrolyte. All experiments were performed in at least three different ionic strengths, ranging from 10^{-3} up to 1 M, in order to determine the common intersection point (c.i.p). If no specific adsorption takes place, i.e. if the supporting electrolyte is indifferent with regard to the oxide, the c.i.p equals the p.p.z.c. As titrants, 0.1 N KOH and HCl, prepared from Merck standard solutions were used. Titrations were performed from pH 4 up to pH 10 in 50 ml volumes containing 1-2 gram of haematite. At these low solid concentrations, the suspension effect [5] was negligible. Therefore, the use of a saltbridge was omitted. The titration cell can be schematically represented as

Ag/AgCl electrode (Schott, B 292)	haematite suspension in KCl solution of variable pH	glass electrode (Schott, N 118)

The air-tight borosilicate glass titration vessels (Schott, 100 ml) were flushed continuously with purified and moisted N_2, in order to purge the solutions from CO_2. Titrants were added by a Metrohm AG-CN 9100 automatic burette. Calculation of the amounts of titrant to be added, addition of titrant, as well as the pH readings were controlled by a HP-85 microcomputer, whose programs were designed such that experiments could be carried out either on a time-basis or on an equilibrium-basis criterion, thus increasing the versatility of the system.

4.3.4 Streaming potential measurements

Streaming potential measurements provide a sensitive method for obtaining electrokinetic data of charged particles. Basically, the equipment used consisted of two pressure-tight polyethylene cylinders connected by a haematite-coated capillary. Exposed glass parts were avoided to prevent silica contamination. One cylinder was connected to a vacuum pump. Pressure reduction in one of the cylinders caused electrolyte solution of known ionic

strength and pH to pass through the capillary, thus establishing a potential difference between two Pt black electrodes positioned in the vessels. The streaming-potential (E_s) was measured with the aid of a high resistance voltmeter (Keithley 616 Digital Electrometer), and converted into the zeta-potential (ζ) using the relation [27, p. 66]

$$\zeta = 4 \pi \eta \kappa_{sp} E_s / \varepsilon P \qquad (\zeta < 50\text{mV}) \qquad (4.1)$$

η being the solution viscosity, ε its dielectric constant, κ_{sp} the specific conductance of the solution, and P the applied pressure difference.

4.3.5 Coating of the capillary

Homodisperse haematite (particle size ≈ 40 nm) was converted from aqueous solution to absolute ethanol by a repeated centrifugation- resuspension treatment. The inner surface of a glass capillary (inner diameter 0.7 mm) was roughened with a steel wire and an aqueous carborundum suspension as an agitating agent. After cleaning, the capillary was filled with the ethanol suspension and dried at 40° C after removal of the excess liquid. This procedure of coating and drying was repeated till a thick haematite coating covered the surface. To prevent the haematite from being washed off due to the rather high shear rates that developed during an experiment, the capillaries were subjected to sintering at 560° C for about 4 hours. The effect of the heat treatment is studied explicitly in this report. The final coating proved to be highly sealed to the supporting glass. An electron micrograph of the coated glass surface is shown in figure 1.

Before every experiment, the coating was etched with concentrated hydrochloric acid, excessively rinsed with water, and stored in 10^{-4} M HCl. The final results proved to be very sensitive to the pretreatment of the capillary. However, when the acid treatment was applied, the results were reproducible within experimental error.

4.3.6 Electrode

Haematite electrodes were designed by coating roughened Pt plates (1x1.5 cm) with sample (a). Coating technique and pretreatment of the electrode prior to use were identical with the procedure described above.

4.3.7 Electrophoresis

Electrokinetic data on non-ignited haematite were obtained with a Zeta-

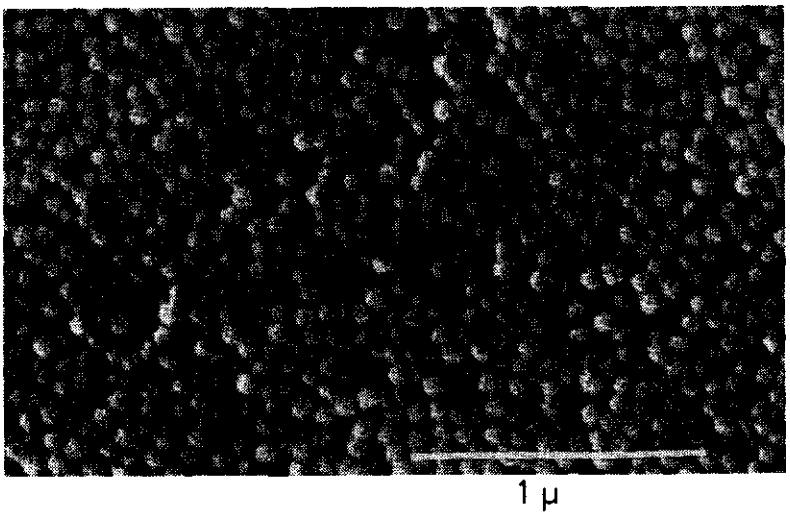

FIGURE 4.1. Scanning electron micrograph of haematite coated glass. Coating sol: Homodisperse haematite, radius 40 nm (sol (a)). Despite the heat treatment the spherical shape of the individual particles remains clearly visible.

sizer II microelectrophoresis equipment provided by Malvern Instruments Ltd. The mobility measurement is based on the Laser-Doppler principle [27]. The equipment allowed extremely rapid measurements so that artefacts due to pH changes in the cell or silica adsorption onto the colloid surface do not interfere with the measurements.

4.4 RESULTS AND DISCUSSION

4.4.1 Time effects and surface charge density

Titration experiments, performed on Breeuwsma's haematite (b) could be carried out on a time base without any indication that changes in the addition criterion influenced the final titration results obtained, as long as after each addition at least 2 minutes equilibration was allowed. Also the titration direction (low to high pH or vice versa) had no effect on the final result. However, very pronounced time effects were observed when such non-equilibrium time base titrations were performed on the coated-Breeuwsma (c), or the monodisperse sol (a). As a consequence, the titration behaviour for those samples did depend to a large extend on the titration direction as is examplified in figure 2 for sol (a). To avoid time effects, all further

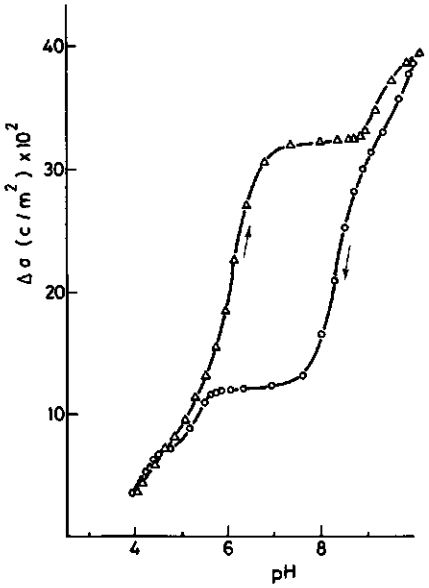

FIGURE 4.2. Surface charge curves of homodisperse haematite (sample (a)), titrated on a time base from low to high pH and vice versa. Time between two subsequent additions of titrant: 2 min. Titrations have been performed in 1.0 M KCl. The charge density is given relative to an arbitrarily chosen reference point.

experiments were performed under equilibrium conditions, defined as the situation where the pH changed less than 0.01 pH unit/ 5 min. Under these conditions, reproducible titration curves could be obtained for all samples.

Equilibrium titration curves, obtained in 0.1 M KCl for the three haematite samples are collected in figure 3. The change of surface charge with pH (charging capacity) of the forced hydrolysis samples ((a) and (c)) exceeds that of the Breeuwsma sol (b), as does the time needed to establish equilibrium under the above criterion: in figure 4 the time to reach equilibrium is shown for titrations starting at low pH values. The slope of the curve is a measure of the time needed to reach the equilibrium situation at each pH. The samples (a) and (c) establish a marked time lag in the vicinity of the pH value where the c.i.p. (indicated by an arrow) is observed. Similar behaviour has been noted before by Parks et. al. [8]. As the morphological characteristics (i.e. size and shape) of the particles in these sols ("coated" and "Breeuwsma") are comparable, differences in titration behaviour must be originated in modifications caused by the coating procedure.

The time effects observed for the forced hydrolysis samples as well as the differences in charging behaviour might be the result of slow, pH induced surface reactions, involving partly amorphous iron oxide precipitates generated in the course of the cleaning procedure. If hydrolysis during the process of formation of the sols is not complete, precipitation of amorphous

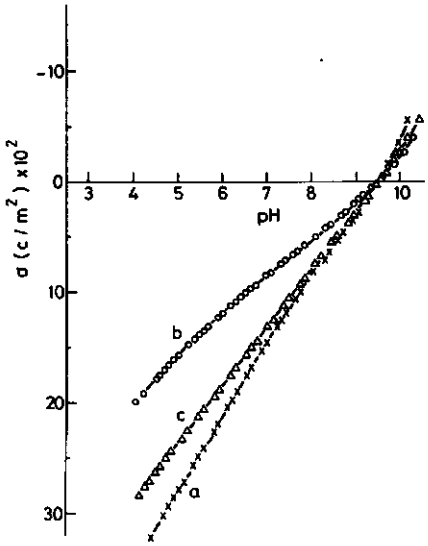

FIGURE 4.3. Equilibrium surface charges of haematite samples (a) *, (b) O, and (c) Δ in 0.1 M KCl. The location of the zero charge axis has been determined by titration of the samples at different ionic strengths. For the sake of clarity, results for other ionic strengths have been omitted.

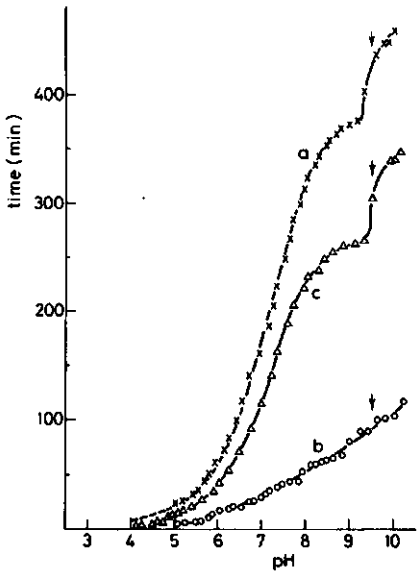

FIGURE 4.4. Cumulative time required for an equilibrium titration. Experiments have been performed in 0.1 M KCl. The initial pH was 4. Titrated samples: Homodisperse haematite (a) *, Breeuwsma haematite (b) O, and coated haematite (c) Δ.

material on the surface might occur. The cleaning procedure following the sol synthesis is usually carried out under conditions (low temperature, pH > 1) which favour the generation of polymorphic iron oxides being accumulated on the particle surfaces. A subsequent autoclave treatment (heating the sols to 150° C for several hours under increased pressure) will convert the amorphous oxides and other crystal modifications to α-Fe_2O_3 [22]. Indeed,

the surface charge of freshly prepared forced hydrolysis haematites changed drastically with autoclaving. It became comparable in behaviour to Breeuwsma's samples which had been subjected to an autoclave treatment in the course of their synthesis procedure. Equilibrium was faster attained and a reduction in the charging capacity down to Breeuwsma's values could be observed. Based on such observations we believe that slow equilibration as well as the absolute value of σ_0 are governed by pH dependent structural changes on the surface involving amorphous (hydr)oxides in addition to modifications of the pristine oxide which might occur as well [7].

4.4.2 The common intersection point

A remarkable difference between Breeuwsma's titration data [5] and titrations performed with sols (a) and (c) (see figure 5) consisted in the location of the common intersection point. It differed by about 1 pH unit

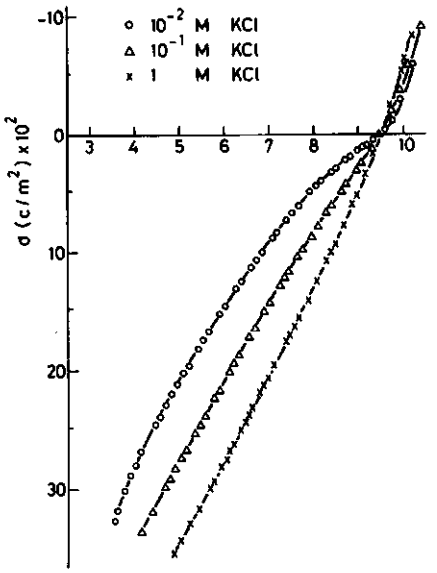

FIGURE 4.5. Equilibrium surface charge of sol (a) for different indicated concentrations of KCl.

(8.5 resp. 9.5). Our experiments with Breeuwsma's original samples (b) confirmed his reported results (see figure 6), provided the haematite was purified by precipitation at pH > 9, or when no substantial purification was applied. However, a shift of the c.i.p. to pH 9.5 occurred when the purification treatment was performed at pH < 8. No changes in the σ_0 (pH) relation were observed when such a sample, purified at low pH was repurified at high pH and titrated again.

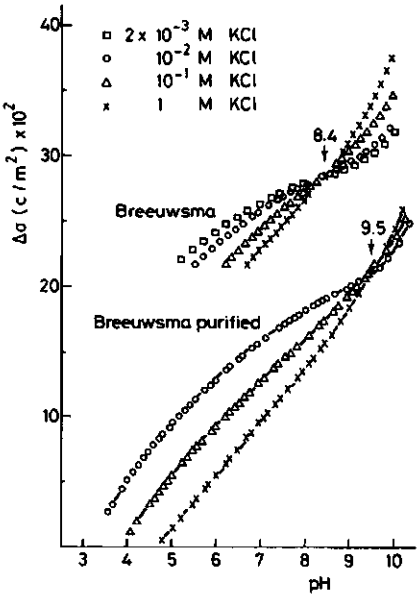

FIGURE 4.6. Surface charge of non-purified Breeuwsma and purified Breeuwsma sol for several indicated concentrations of KCl. Charge density is given relative to an arbitrarily chosen reference point. P.z.c. values are indicated by the arrows.

Considering the fact that Breeuwsma pointed to the presence of ionic impurities in his samples, in particular Ca^{2+} and Mg^{2+}, which proved to be strongly retained by the oxide, it is likely that the shift in the c.i.p. has to be attributed to the specific adsorption of these cations to the surface. Cleaning (or titration!), performed at "low" pH, i.e. below the c.i.p. will cause the expulsion of the positive ions due to electrostatic repulsion, whereas treatment above the c.i.p. will have no effect. Titrations with insufficiently purified sols, containing traces of ionic contaminants with a high specific affinity for the surface are virtually performed in a mixed electrolyte, even though only one indifferent electrolyte is added as the background. Consequently, the common intersection points reported by Breeuwsma are more likely to be equal compensation points (a term, defined by Lyklema [9]), i.e. the pH to the left of the p.p.z.c where the surface charge is so positive that the chemical affinity of Ca^{++} and Mg^{++}-ions for the surface is just compensated by electrostatic repulsion.

The c.i.p. obtained for purified sols equals the i.e.p. found independently by electrokinetic experiments: figure 7 shows a plot of the electrophoretic mobility vs. pH for sample (a) in 10^{-2} M KCl. The i.e.p. is in good agreement with the c.i.p. This identity indicates that KCl is an indifferent electrolyte for haematite (a) and that both the c.i.p. and the i.e.p. coin-

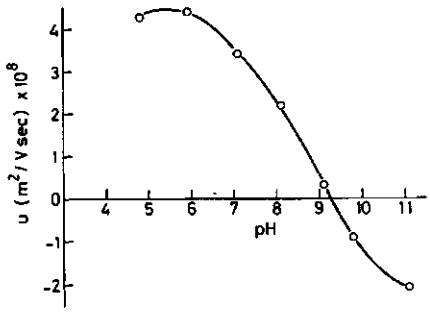

FIGURE 4.7. Electrophoretic mobility of sol (a) vs. pH in 10^{-2} M KCl.

cide with the p.p.z.c.. Iso electric point values for haematite reported in literature [7,21,24,25] vary widely. Usually they are rather low and show little resemblance with commom intersection points. The cause for such deviations might be the binding of small amounts of multivalent ions to an extend, determined by the conditions of preparation and cleaning of the sol. Comparsion with the present results indicates that most of the i.e.p. and p.z.c. (= c.i.p.) values tabulated in literature for haematite should be regarded with reserve.

Tying on to results presented under the heading "time effects", it should be stressed that the location of the c.i.p. for a given, non contaminated, haematite is rather insensitive to pH induced structural modifications of the oxide surface, probably due to compensating effects on pK_a and pK_b. The observed numerical values range from 9.0 to 9.5, even though the titration behaviour of different non-autoclaved samples differs drastically with respect to capacitance and equilibration time. Model calculations of p.p.z.c. values vary between the same close limits, independent of whether the charging mechanism is described by assuming a fixed stoichiometry of the haematite surface throughout the titrations (an approach adapted by Yoon [10]) or by pH-dependent structural changes [7]. We therefore believe, in contrast to previous reports, that the real p.p.z.c. value of haematite is located in the vicinity of pH 9.5.

4.4.3 Influence of heating

The hydrous material (amorphous iron oxide, FeOOH) which is considered to be present on the surface of oxide precipitates, formed by polymerisation and oxolation in aqueous solution, will be lost during a treatment of drying and/or heating. A heat treatment involving temperatures of 500-600° C results in complete dehydration of the haematite [26] and might induce

changes in the stoichiometry of the crystal. If subsequently the dehydrated oxide is brought into contact with an aqueous solution, the surface will rehydrate to some extent and there is evidence that it will establish the properties of α-FeOOH [7].

The effect of such a heat treatment on the surface charge and electrokinetic characteristics of haematite is demonstrated in figures 8 and 9 which show the dependence of the charge density (fig. 8) and the zeta potential (fig. 9) of ignited samples on pH for several concentrations KCl. The

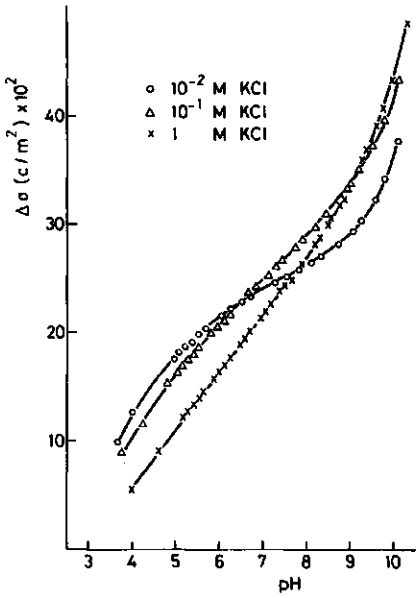

FIGURE 4.8. Surface charge of the heated haematite (b) for several indicated ionic strengths.

observed intersection points of the titration curves and the obtained i.e.p.'s support the established idea that any treatment which causes extensive surface dehydratation results in a more acid p.p.z.c. and i.e.p. [7,16,17].

The titration results collected in figure 8 show that the intersection point values for different pairs of electrolyte concentrations do not coincide. Additional experiments showed that the reproducibility of titrations performed with freshly heated and subsequently repurified sols was extremely poor. The absence of one c.i.p. indicates that the surface properties of heated haematite too are subjected to pH-induced modifications. If irreversible changes occur in the course of a titration process then the titration curves obtained with freshly prepared heated oxide will not be comparable

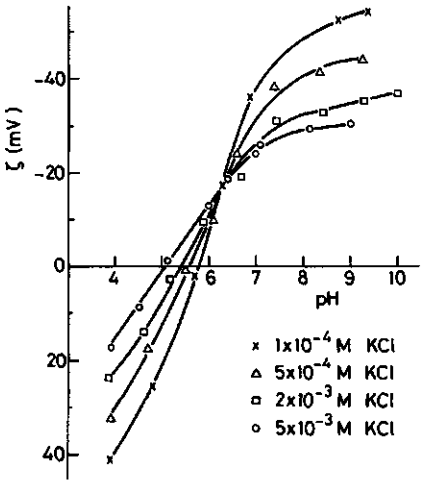

FIGURE 4.9. Zeta potentials obtained by steaming potential measurements on coated and heated haematite capillaries at different pH values for several ionic strengths.

with subsequent curves. That modifications do occur is also emphasized by the irreversibility in electrokinetic behaviour observed, when the Zeta potential vs. pH curve of a freshly etched capillary is compared with the same dependence of a second run. (see figure 10). Obviously the pretreatment (titration to high pH values) has a marked effect on the electrochemical behaviour of the oxide.

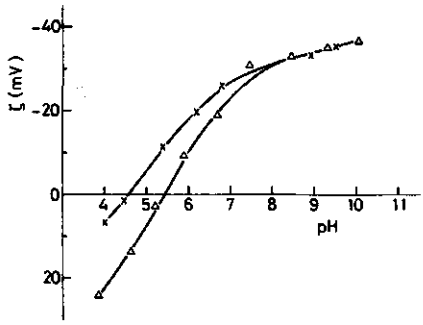

FIGURE 4.10. Zeta potential vs. pH for a freshly etched haematite-coated capillary (Δ) and the same capillary after the performance of one titration cycle (*).

An additional factor affecting the location of the intersection points of the titration curves is specific adsorption: the decrease of the i.e.p. with increasing electrolyte concentration points to the role of Cl^- in this respect. The affinity of chloride for the haematite surface explains also why the intersection points of figure 8 differ in magnitude with the isoelectric points of figure 9: according to basic double layer concepts, any specific (excess) anion adsorption will cause the intersection point to

shift to higher pH and the i.e.p. to lower pH. It should be emphasized that specific adsorpion of Cl^- on the heated haematite sol is clearly present, but the electrophoretic study on the non heated haematite (a) (see above) indicated that no specific adsorption occured on such samples. Apparently there are profound differences between the interfaces of samples whose bulk material is crystallographically identical. The amounts of Cl^- at the interface are too small as to be detectable by classical analytical techniques. However, shifts of intersection points and i.e.p.'s are sufficiently sensitive to indicate their presence.

The use of oxide electrodes is in principle a powerfull tool to obtain additional direct information about the electrochemical properties of the oxide under investigation. In figure 11, the dependence of the potential of a heated haematite electrode in $5x10^{-3}$ M KCl on pH is depicted. Nernstian behaviour could be observed over many pH units. Deviations from the Nernstian slope occur only at rather low pH values. Though the result looks promising, extensive use of the electrodes in the described electrochemical studies was avoided, as the electrodes showed very long equilibration times and haematite surfaces heated up to 560° C are not really representative for the usually encountered heamatite hydrosols. The development of better suited electrodes was not the primary aim of our study, therefore no further attention has been paid to this item.

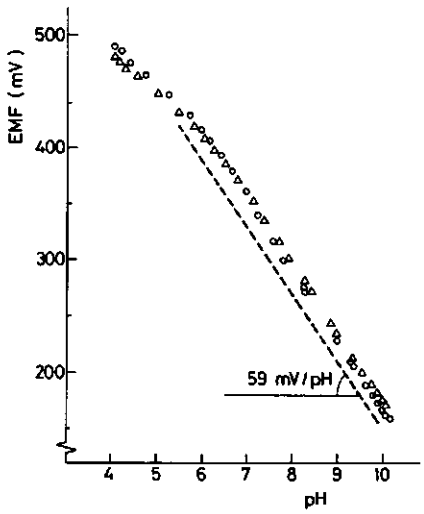

FIGURE 4.11. The electromotoric force (E.M.F.) of a haematite electrode in $5x10^{-3}$ M KCl vs. pH at 20°C. In the figure the results of two different runs are represented.

4.5 CONCLUSIONS

The results discussed in this paper are to some extent a conformation of already reported insights. They emphasize once more that the crystal structure of the bulk phase is not the exclusive parameter determining the interfacial electochemical behaviour of an oxide. Factors like purification or pretreatment of aqueous sols or dried material might be equally important as was established by the following observations:

- Slight alterations in the pH during the cleaning of the sol have a pronounced influence on the location of the common intersection point found by titration.
- Autoclaving of an aqueous haematite sol, not previously heated, does not influence the location of the c.i.p., but it does change the capacitance and the equilibration time. The i.e.p. and c.i.p. of well-purified (non-heated) haematite samples agreed very well and indicate a p.p.z.c. value for haematite of 9.5.
- A heat treatment (500-600° C) applied to dried suspensions causes the c.i.p. to decrease drastically. This decrease is, at least on the timescale of the experiment, irreversible.
- Dried, heat treated and subsequently resuspended samples show some specific affinity for Cl^- which could not be detected for the non treated samples: their iso electric points, determined by microelectrophoresis, agreed well with point of zero charge values obtained by potentiometric titrations.

The observed phenomena are probably closely connected to structural changes at the haematite surface, involving amorphous iron (hydr)oxide precipitation and modification of the outer layer of the crystal material, which take place if the pH in the sol is altered. Though such structural changes seem to occur independent of the pretreatment of the sample, they do not lead to an unique surface structure for different pretrated oxides, at least not on the timescale of the experiments.

4.6 ACKNOWLEDGEMENTS

We wish to thank Erna Rouwendal for the kind performance of the streaming potential measurements and some of the titrations. Ronald Wegh is acknowledged for designing the titration equipment and for providing first aid

when bugs in the titration programme threatened to ruin an experiment. Malvern Instruments Ltd. is kindly acknowledged for their cooperation concerning the use of the Zetasizer II.

4.7 REFERENCES

(1) Douwsma, J., thesis, University of Utrecht, The Netherlands (1979).

(2) van der Woude, J.H.A., thesis, University of Utrecht (1983).

(3) Matijević, E., and Scheiner, P., J. Colloid Interface Sci. **63**, 509 (1978).

(4) Matijević, E., "Properties of Colloidal Corrosion Products and their Effects on Nuclear Plants.", Energy Res. Abstr. **8**, Abstr. No. 5039 (1983).

(5) Breeuwsma, A., thesis, Agricultural University Wageningen, The Netherlands (1973).

(6) Horvath, G.L., Snellman, M. and Rämo, E.G., in "Water Chemistry of Nuclear Reactor Systems, 2.", British Nuclear Energy Society **235** (1981).

(7) Parks, G.A., Chem. Rev. **65**, 177 (1965).

(8) Parks, G.A. and de Bruyn, P.L., J. Phys. Chem. **66**, 967 (1962).

(9) Lyklema, J., J. Colloid Interface Sci. **99**, 109 (1984).

(10) Yoon, R.H., Salman, T. and Donnay, G., J. Colloid Interface Sci. **70**, 483 (1979).

(11) Lyklema, J., Croat. Chem. Acta **43**, 249 (1971).

(12) Onoda, G.Y., and de Bruyn, P.L., Surface Sci. **4**, 48 (1966).

(13) Healy, T.W., and White, L.R., Advan. Colloid Interface Sci. **9**, 303 (1978).

(14) James, R.O., and Parks, G.A., in "Surface and Colloid Science", Vol. **12**, Matijević, ed., Plenum Press, New York and London, 119, (1982).

(15) Ardizzone, S., Siviglia, P. and Trasatti, S., J. Electroanal. Chem. Interfacial Electrochem. **122**, 395 (1981).

(16) Berubé, Y.G., and de Bruyn, P.L., J. Colloid Interface Sci. **27**, 305 (1968).

(17) Johansen, P.G., and Buchanan, A.S., Aust. J. Chem. **10**, 398 (1957).

(18) Ardizzone, S., Biagiotti, R., and Formaro, L., J. Electroanal. Chem. Interfacial Electrochem. **135**, 167 (1982).

(19) Penners, N.H.G., and Koopal, L.K., Colloids and Surfaces, submitted.

(20) Breeuwsma, A. and Lyklema, J., Discuss. Faraday Soc. **52**, 324 (1971).

(21) Koutsoukos, P.G., Norde, W., and Lyklema, J., J. Colloid Interface Sci. **95**, 385 (1983).

(22) Weiser, H.B., and Milligan, W.D., J. Phys Chem. **39**, 25 (1935).

(23) Westall, J. and Hohl, H., Advan. Colloid Interface Sci. **12**, 265 (1980).

(24) Scheiner, P., thesis, Clarcson College of Technology (1979).

(25) Chang, H.C., Healy, T.W., and Matijević, E., J. Colloid Interface Sci. **92**, 469 (1983).

(26) Morimoto, T., Nagao, M., and Tokuda, F., J. Phys Chem. **73**, 243 (1969).

(27) Hunter, R.J.,"Zeta Potential in Colloid Science: Principles and Applications", in "Colloid Science: A Series of Monographs, Vol. 2", Academic Press, London (1981).

V. THE EFFECT OF PARTICLE SIZE ON THE STABILITY OF HAEMATITE (α-Fe_2O_3) HYDROSOLS

5.1 ABSTRACT

In order to investigate the influence of particle size on colloid stability, flocculation experiments have been performed with a series of homodisperse haematite sols containing particles from 37 to 350 nm radius. The pronounced dependence of stability on particle size, predicted by classical DLVO theory, could not be observed; although the critical coagulation concentration changed with particle size and showed a minimum at radii of about 180 nm, the stability ratio W proved to be virtually size independent. However, the observed effects could be explained with the concepts provided by the DLVO theory if some extentions, assuming a distance of minimum approach between coagulating particles and redispersion are incorporated. Model calculations show that deviation from sphericity might be another factor responsible for the differences in coagulation behaviour between the different model systems.

5.2 INTRODUCTION

5.2.1 General background

Due to the impact on many fields of science and technology, the properties of submicron dispersions have been studied extensively since the beginning of this century. Substantial progress in colloid research has been made with the development of the DLVO theory [1,2] which attributes the interactions between two colloid particles to the antagonistic action of van der Waals attraction and electrostatic repulsion.

In the light of this theory, many aspects of colloid behaviour, for instance the pronounced influence of electrolyte concentration and counter ion valence on stability are clearly understood. In addition, a framework was provided on which models concerning the influence of particle size on colloid stability could be developed [3,4]. These early models describe the coagulation proces in terms of the energy barrier (V_{max}) that is experienced by particles during approach. As a consequence of this barrier concept, under slow coagulation conditions, small particles should exhibit more rapid

coagulation then larger ones, whereas the critical coagulation concentration (c.c.c.) is size independent. In addition, coagulation should be irreversible, i.e. repeptisation of a coagulated system by decreasing the electrolyte concentration or by moderate stirring should not occur.

Even though a substantial amount of experimental work has been devoted to the influence of particle size on colloid stability, no exclusive proof has been obtained for the validity of the theory in this respect. On the contrary, experimental results are contradicting: as mentioned by Reerink and Overbeek [3], for monodiperse gold sols a decrease, an increase as well as an independence of colloid stability on particle size have been reported. Selenium sols show rather large differences in coagulation rate at nearly the same particle size [5], and no conclusive trends could be observed for differently sized AgI [3] or silica [6] sols.

As, due to the ill defined shape of the sol particles, the possibility exists that the contradictory results are caused by deviations from sphericity and contributions of surface irregularities rather than by differences in size, later more systematic research dealt with latices as model systems for size effect investigations. With those systems a decrease in stability with increasing particle size [7,8] or increase followed by decrease [9,10] have been reported. Such results suggested that particle coagulation is not restricted to the primary minimum but could also occur in the secondary minimum (which is rather pronounced for the usually larger sized latices). By considering the possibility of secondary minimum coagulation in already available models [11], many of the observed trends, i.e. changes in c.c.c. with size and coagulation reversibility [10,12] could be accounted for satisfactorily. However, the predicted size dependence in the slow coagulation range has not yet been found experimentally. On this point the encompassing DLVO theory seems to have its limitations.

In recent years the awareness grew that at short distances of approach (~ 1-2 nm), hydration forces (forces of a repulsive nature, originating in the repulsive action of hydrated adsorbed counterions) play a dominant role in balancing the counteracting forces which determine the stability of colloids [45-47]. They might account for part of the difference in behaviour predicted by theory and that encountered in practice.

Even though in the past much progress has been made in the understanding of size effects on colloid stability and especially in the sixties and early seventies the interest of many colloid chemists focussed on this subject,

the field remained unexplored over the past decade. One of the causes of this recess might be the limited availability of model systems which, besides the ubiquituous latices, suit the needs for systematic size studies: particles have to be spherical, extremely homodisperse, they must cover a large range of sizes and should have comparable surface properties. The last mentioned requirement demands that all sols, irrespective of their size have to be prepared by the same procedure without any alteration of synthesis conditions. Due to recent demands from technology, concerning fields like catalysis, corrosion research and the development of new systems for energy conversion, the synthesis of colloid model systems has received new impulses, and sols meeting the mentioned requirements have become available [13-15].

In an earlier report [16] (see chapter 2) we described the synthesis of homodisperse haematite (α-Fe_2O_3) sols with spherically shaped particles, synthesized under identical conditions covering a large size range and insight has been gained in their optical [17] and interfacial [18] properties (see chapters 3 and 4). The present paper gives an account of some stability experiments carried out using these sols, focussing attention both to energetic stability requirements as well as to coagulation kinetics. Special emphasis is given to the influence of particle size on stability and results are explained in the light of a modified DLVO theory.

5.2.2 Basic aspects of colloid stability

(a) Energetic considerations: According to the DLVO theory, the total potential energy of interaction (V_t) between two spherical colloid particles divided by a distance H is defined as

$$V_t(H) = V_R(H) + V_A(H) \qquad (5.1)$$

The term V_R (free energy of repulsion due to electrolyte dependent double layer interaction) is related to the Stern layer potential Ψ_d, the reciprocal Debye length κ, the particle radius r and the Stern layer thickness Δ by an equation derived by Bell et.al. [20] and modified by de Wit [19]:

$$V_R = 64\ \pi\ \varepsilon_0\ \varepsilon_r \left(\frac{KT}{ze}\right)^2 \left(\frac{r+\Delta}{s'}\right)\left[\tanh\left(\frac{ze\Psi_d}{4KT}\right)\right]^2 \exp[-\kappa(r+\Delta)(s'-2)] \qquad (5.2)$$

ε_0 is the dielectric permitivity of vacuum, ε_r the relative permitivity of water, z the valence of the counterion, e the elementary charge, k the Boltzman constant and T the absolute temperature. In this equation the meaning of the reduced Stern layer distance s' (= $R/(r + \Delta)$) is explained in fig. 1.

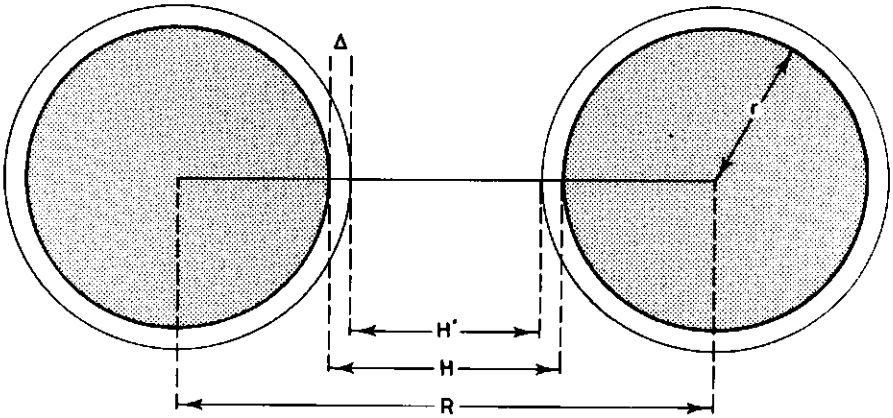

FIGURE 5.1. The distances of interaction between two colloid particles: R = distance between the particle centres. H = closest distance between the particle surfaces H' = effective distance for particle repulsion. The reduced Stern layer distance s' is given by $s' = R/(r + \Delta)$.

For not too small interparticle distances, V_A (energy of attraction originating in retarded London- van der Waals dispersion forces) can be approximated by [21,11]:

$$V_A = -\frac{A\ r}{12\ H}\left[\frac{1}{(1 + 1.77\ p_0)}\right] \qquad (5.3)$$

Where A is the Hamaker constant, $p_0 = 2\pi H/\lambda$ and λ is the wavelength corresponding to the intrinsic oscillations of the atoms in the particles, which cause the retardation. In the computations reported in this paper, λ has been chosen to be 100 nm. Equation (3) is valid for $p_0 < 2$, a requisite met for separations up to about 30 nm.

A plot of the total energy of interaction V_t as a function of the distance of separation H between the particle surfaces exhibits some distinct features (see fig. 2): a primary maximum (V_{max}) at rather small separations and a secondary minimum (V_{sec}) at larger separations, whose magnitudes

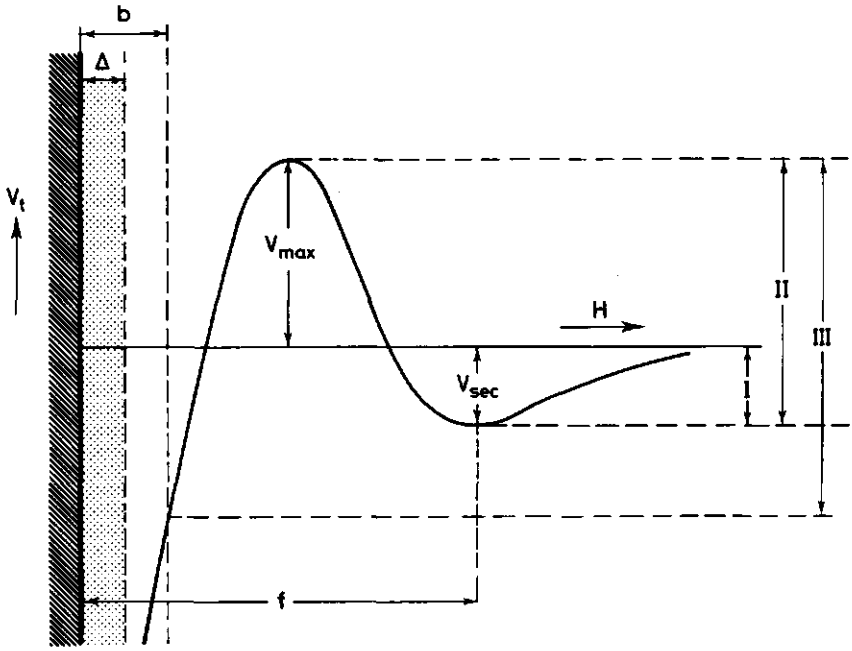

FIGURE 5.2. Total interaction energy between two colloidal particles vs. distance H. Δ = Stern layer thickness. b, the distance of closest approach is assumed to be 2Δ. f = trapping distance for secundary minimum flocculation. I = depth of the secundary minimum. II = barrier energy for primary minimum flocculation. III = redispersion barrier energy.

depend on the particle size, electrolyte concentration as well as Stern layer potential. Theoretically, the distance of approach H between two particles can be reduced to zero. However, in recent years evidence on repeptisation support the idea that coagulating particles remain separated by a finite distance b [22]. The cause for such a distance of closest approach might be the already mentioned hydration forces or an irregular particle-solution boundary. To avoid complicating assumptions about the potential drop in the Stern layer, in the calculations to be reported the distance b has been assumed equal to 2Δ (being therefore comparable with the extention of the hydration forces). Although this choise is clearly arbitrary, the advantage of parameter reduction outweights this objection. In addition, it does not affect the principle of the analysis to be presented.

A sol is assumed to be stable, if the secundary minimum V_{sec} is too shallow to trap encountering particles on a distance f, and the effective potential barrier III (= V_{sec} + V_{max}) is high enough to avoid primary minimum coagulation on a distance b = 2Δ. As will be evident from the steep slope of the interaction energy at very close distances of approach,

repeptisation, which is closely related to the magnitude of the barrier III, will strongly depend on the distance of closest approach b.

(b) Coagulation: Aggregate formation is the result of encounters of two particles. Its rate should therefore be determined by the laws governing a bimolecular reaction: The decrease in particle number N_t with time t equals

$$dN_t/dt = k_r N_t^2 \qquad (5.4)$$

If no interaction exists between the two particles except a short range force leading to permanent contact after encounter, the rate constant for coagulation k_r, which under those circumstances is determined by the Brownian motion of both particles is given by [23]

$$k_r = 16 \pi D r \qquad (5.5)$$

where D is the diffusion coefficient of the particles. As for spherical particles $D = kT/6\pi\eta r$, where η is the medium viscosity, equation (5) can be written as:

$$k_r = 8 k T/3 \eta \qquad (5.6)$$

The rate constant is independent of particle size, which is due to the fact that the slower Brownian motion of the larger particles is exactly compensated by their larger collision cross sections.

However, as pointed out before, in a real sol particle interactions do exist which exert their influence during approach. Therefore, attention has been focussed on the incorporation of interaction contributions in Smoluchowski's [23] kinetic approach [24]. These efforts resulted in a definition of colloid stability in terms of the stability ratio W:

$$W = k_s/k_r \qquad (5.7)$$

k_s, the rate constant for slow coagulation is determined by the dependence of the total interaction energy V_t on the distance between two particles. k_r is the rate constant for rapid flocculation, that is: under conditions where repulsive forces can be neglected, i.e. $V_t = V_A$. The last mentioned condition is encountered at high electrolyte concentrations.

Later on, the stability ratio concept was elaborated in more detail [25-27] by taking into account that the approach of two particles is slowed down due to hydrodynamic resistance. Because of this "squeezing resistance" the diffusion coefficient becomes distance dependent:

$$D(u) = D/\beta(u) \tag{5.8a}$$

and

$$k_r = 16\ \pi\ D(u)\ r \tag{5.8b}$$

D(u), the real diffusion coefficient is related to the unperturbated one D by a correction factor $\beta(u)$, whose value can be approximated by [27]:

$$\beta(u) \simeq (6u^2 + 13u + 2)/(6u^2 + 4u) \tag{5.9}$$

In the presence of a Stern layer, the reduced interparticle distance u (= H/r, see fig 1) has to be replaced by $u' = H'/(r + \Delta)$ [19]. That coagulating particles experience some rate decreasing resistance has been substantiated experimentally by measuring the rate of rapid coagulation of homodiperse sols [12,28-31]. Experimental values are in the range of $2\text{-}3\times10^{-18}$ m^3/s, which is significantly lower then the Von Smoluchowski value ($\simeq 6.1\times10^{-18}$ m^3/s). Furthermore, the experiments showed that the rate of coagulation is independent of particle size [28].

By incorporation of the hydrodynamic drag in the definition of the stability ratio, W can be written as [27]:

$$W = \frac{k_s}{k_r} = \frac{\int_0^\infty \frac{\beta(u')}{(2+u')^2} \exp\left(\frac{V_t}{kT}\right) du'}{\int_0^\infty \frac{\beta(u')}{(2+u')^2} \exp\left(\frac{V_A}{kT}\right) du'} \tag{5.10}$$

Since V_t is proportional to the particle radius, with increasing particle size the stability of a sol will increase for primary minimum coagulation, but will decrease when secondary minimum coagulation is concerned. Which mechanism is operative depends on particle size as well as on the

electrolyte concentration. For certain size- and electrolyte concentration ranges, the two coagulation states might occur simultaneously, complicating any theoretical analysis.

5.3 EXPERIMENTS AND METHODS

5.3.1 Sols

The homodisperse haematite sols have been synthesized according to a method outlined previously [16] (see chapter 2). They proved to be homodisperse (standard deviation of the particle radius < 5 %). Some properties of the samples are compiled in table 1. Besides the light scattering radius and

TABLE 1: Some properties of the sols.

SOL	RADIUS	r_w/r_n	pH	WAVELENGTH
A	37	1.034	3 - 8	800
B	86	1.015	4	400
C	134	1.017	4	400
D	173	1.009	4	400
E	225	1.009	4	400
F	282	1.006	4	400
G	352	1.005	4	400

measuring conditions (solution pH and wavelength of the light used for tubidimetric monitoring), the ratio between weight and number average radius is compiled. All experiments described were performed with dilute sols (concentration 0.06-0.5 mg/ml, depending on particle size) whose pH was adjusted by the addition of HCl or KOH.

5.3.2 Stability measurements

(a) Coagulation kinetics: experiments performed with the sol containing the smallest particles (r=37 nm) were carried out with a Durrum-Gibson stopped flow spectrophotometer at a wavelength of 800 nm. In the experimental set-up, the original oscilloscope recording unit was replaced by a HP-85 minicomputer in combination with a Fluke 8810 A voltmeter, and a Fluke 1102

IEEE translator. This set-up enabled the recording of the extinction course with time, as well as simultaneous determination of the initial slope. Every determination was repeated 5-8 times to improve the significance of the final data.

As the optical system of the stopped flow apparatus was not suited for the optical requirements to be met with sols containing bigger particles, stability measurements concerning larger sizes were done with a Varian DMS 80 spectrophotometer at 400 nm. For this purpose, the instrument was equipped with a 1 cm cylindrical cel and a magnetic stirrer, enabeling homogenisation of sol and electrolyte within 1 s. On t=0, coagulation was initiated by injection of 0.75 ml electrolyte solution to 0.75 ml sol using a Gilson pipetman. Also in this set up the determinations were repeated up to 7 times in order to improve the results. As with the stopped-flow, data recording and -processing was performed using the allready mentioned HP-85 with periphery equipment. All stability experiments were carried out with KCl as the coagulant. By continued stirring after the homogenisation of sol and added electrolyte, orthokinetic conditions (coagulation under shear) could be maintained. However, if after the homogenisation the stirrer was stopped, perikinetic (Brownian) coagulation prevailed.

(b) c.c.c. and i.e.p. determination by titration: in order to locate the c.c.c. at a certain pH, or the position of the iso electric point (i.e.p.) at a fixed electrolyte concentration a turbidity titration method was developed. The basic equipment used in this method was again the Varian DMS 80 spectrophotometer equipped with a cylindrical cuvette, magnetic stirrer, combined pH/Ag/AgCl reference electrode (Schott N 61) and HP-85 assembly as the recording-processing unit. After fixed intervals, titrant (KCl or KOH) was added to 2.0 ml sol, and after homogenisation the derivative of the extinction course versus time curve was determined. A final graph of dE/dt vs. the electrolyte concentration or pH provided direct information about the location of the c.c.c. or i.e.p. When possible time effects were taken into accout by performing the described experiments with different interval lengths, the titration method proved not only to be a quick, but a reproducible technique as well. However, it could only be used as an additional technique to the initial slope measurements, as no significance could be attached to the absolute dE/dt values due to the different "initial" aggregation state at each titrant addition.

5.3.3 Turbidity data analysis

The turbidity (τ) of a coagulating sol, directly after the initiation of the coagulation process (i.e. when aggregates beyond dimers can be neglected) is related to the specific turbidity of the monomers and dimers by the expression:

$$\tau(t) = \tau_m C_m + \tau_d C_d \qquad (5.11)$$

Here, τ_m and τ_d are the specific turbidities of the monomers and dimers respectively and C_m and C_d are their weight concentrations. According to Von Smoluchowski's theory [23], the weight concentration of an i-mer depends on its weight G_i, the initial particle concentration N_0 and the coagulation time $t_{\frac{1}{2}}$ (time in which N_0 is reduced by a factor 2) as follows:

$$C_i = \frac{(t/t_{\frac{1}{2}})^{i-1} N_0 G_i}{(1 + t/t_{\frac{1}{2}})^{i+1}} \qquad (5.12)$$

For $t \ll t_{\frac{1}{2}}$ (condition met for initial coagulation), taking into account that $t_{\frac{1}{2}} = 2/(k_{11} N_0)$, where k_{11} is the rate constant for dimer formation, it can be deduced that

$$(dE/dt)_o = N_o^2 k_{11} G_m [\tau_d - \tau_m] \qquad (5.13)$$

Equation (13) links turbidimetric data ($[dE/dt]_o$) to kinetic parameters. N_0, G_m and τ_m are known parameters, so k_{11} can be calculated from the measurements if τ_d is known. Unfortunately τ_d is hard to access. For latex scatterers an analysis for the calculation of τ_d has been developed [32], introducing form-factors in the Raleigh- Gans- Debye (R.G.D.) scattering theory [28]. However, the R.G.D. theory is valid only if the refractive index of the scatterers is close to the index of the surrounding medium and hence it is not applicable to aqueous haematite suspensions. If the assumption is made that a dimer acts as a homogeneous, spherical scatterer, equivalent in volume to two monomers, τ_d can be calculated using the rigorous Mie theory [17]. Such an approach has been adapted before in the stability analysis of latex sols [9], giving satisfactory results.

The validity of the "coalescing sphere" model, outlined above, is

questionable for haematite. However, the measuring wavelength could be chosen such that the contribution of the monomers to the turbidity exceeds that of the dimers, limiting the impact of the approximation on the final result. In the analysis of the kinetic data to be described in the next section, the "coalescing sphere" model (model 1) has been applied together with a second model based on the assumption that a dimer is optically equivalent to a sphere having twice the radius of a monomer (model 2). The reality will be somewhere between these two extremes.

5.4 RESULTS

5.4.1 Stability

Some typical results of the titration method are compiled in fig. 3, showing the coagulation velocity (expressed in terms of dE/dt) as a function of pH (a) and electrolyte concentration (b). In a coagulating system dE/dt is not constant because of changes in aggregate sizes in the course of time. Therefore, the increase of dE/dt due to an increasing coagulation rate is partly counteracted, giving rise to a maximum in the case of variable electrolyte concentration (fig. 3(b)). For this reason it was mandatory to perform titrations at different speeds.

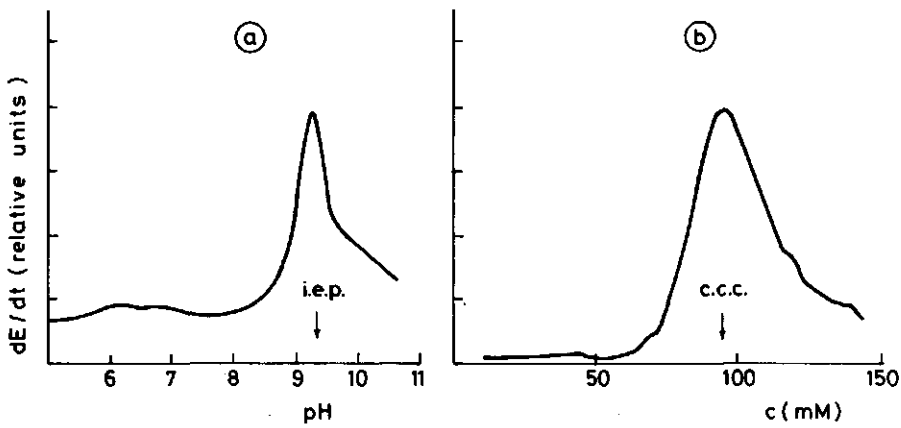

FIGURE 5.3. Some typical results obtained with the titration method. The coagulation velocity (in terms of dE/dt) is given as a function of pH at a fixed electrolyte concentration of 10^{-3} M KCl (a) and of electrolyte concentration at a fixed pH of 4 (b). Experiments were performed with sol A, having a concentration of 0.12 mg/ml.

pH titrations have been performed with all sols compiled in table 1. Though the procedure provides no exhaustive information about the values of the Stern layer potentials of the different sols, location of the i.e.p. is a good measure of the surface properties of the different samples. All determined i.e.p. values proved to be equal within the experimental error. We therefore assume that the particle size is the only variable for the sols under otherwise identical conditions.

In fig. 4, the rates of coagulation (expressed as $[dE/dt]_0$) are shown as a function of the electrolyte concentration for two different particle sizes (37 and 173 nm). Values are determined with the initial slope method. After the concentration of maximum rate of coagulation is reached, the rate relating to the small particles decreases again, whereas for bigger particles, more or less a plateau value is attained. As all exhibited points refer to initial slopes, the observed effects cannot be attributed to differences in aggregation state as might be the case in the titration method mentioned above.

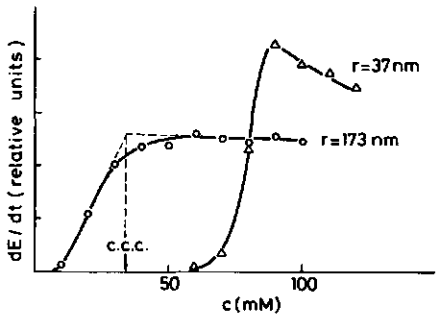

FIGURE 5.4. Initial slope measurements for sol A (r = 37 nm) and D (r = 173 nm). Experiments were perfomed at pH 4 with concentrations of 0.10 (A) and 0.15 (D) mg/ml.

The magnitude of the stability increase at electrolyte concentrations exceeding the c.c.c. as observed for sol A proved to be pH dependent. The more the pH at which an experiment was performed deviated from the p.z.c., the more pronounced the effect (see fig. 5). In addition, the maximum rate of coagulation increased drastically with increasing pH-p.z.c. difference.

Curves like those pictured in fig. 4 were used to determine the c.c.c. by interpolation from the dependence of the flocculation velocity on the electrolyte concentration in the slow- and fast flocculation range as indicated in the figure. The c.c.c. values obtained in this way are shown in fig. 6 as a function of the particle size. For sake of comparsion, c.c.c. values obtained with the titration method are incorporated. With increasing

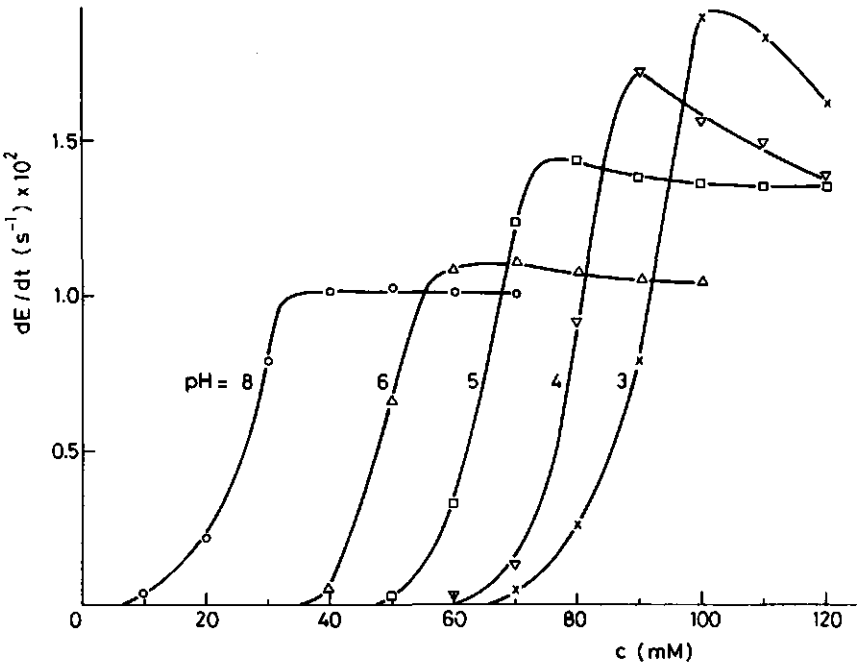

FIGURE 5.5. Initial slope measurements performed with sol A at different pH values. Sol concentration: 0.10 mg/ml.

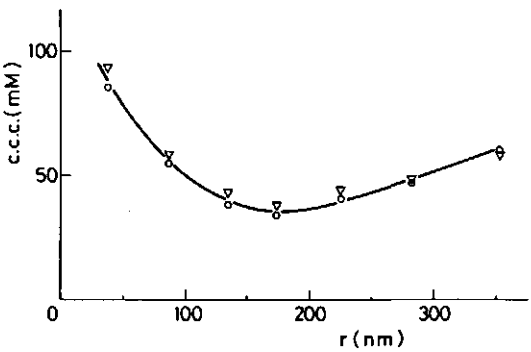

FIGURE 5.6. Dependence of the initial coagulation concentration on particle radius. Data obtained with the titration method (∇) are incorporated together with points derived by interpolation from initial slope vs. electrolyte concentration curves (0). Experiments were performed at pH 4.

particle size the c.c.c. value first decreases, passes through a minimum and then increases again. Even though the absolute c.c.c. values might be open to some doubt due to the limited accuracy of the interpolation procedures applied, the trend will be correct.

In analogy with the procedure followed by other authors [3] the experimental stability curves in fig.7 are expressed as log W vs. log c. The slopes of the curves in the slow coagulation range are roughly the same,

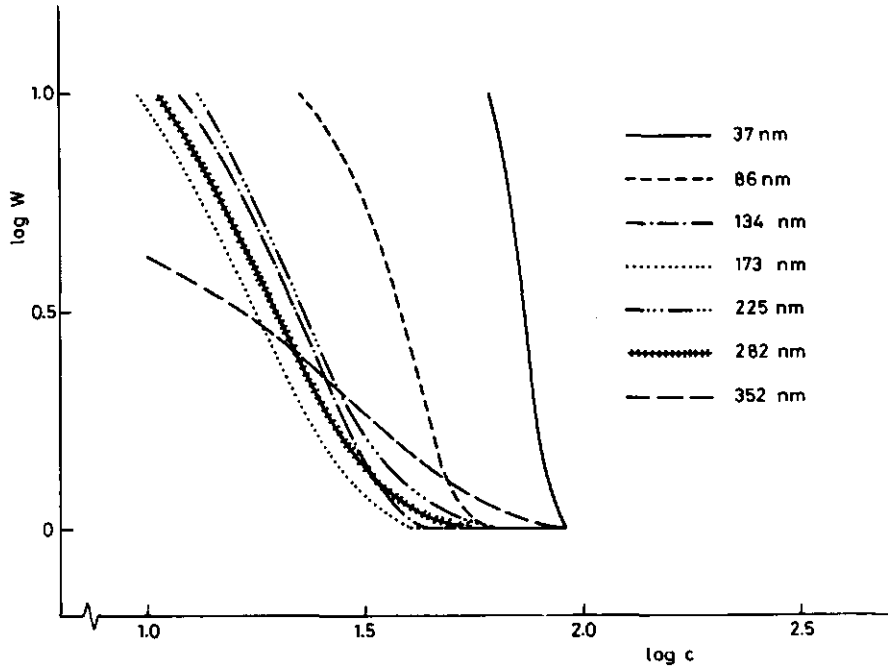

FIGURE 5.7. Log W vs. log c plots for heamatite sols A - G coagulated at pH = 4. The radii of the particles in the individual sols are shown.

except for the biggest particle size. The size dependence expected according to the DLVO theory, i.e. a slope increasing with particle size in the case of primary minimum coagulation is not observed.

5.4.2 Coagulation kinetics

According to the equations (4) and (13), the initial rate of coagulation (i.e. initial dE/dt value) is proportional to the square of the particle concentration in the sol, N_o^2. That this is indeed the case is exemplified in fig. 8 in which the initial slope of the E-t curves is plotted vs. the square of the sol concentration for a system containing particles of 37 nm (sol A).

Assuming that dimers can be regarded as Mie scatterers, according to the models (1) and (2) outlined in the experimental part (5.3.3), eqn. (13) can be used to calculate the coagulation rate constant k_{11} from initial slope data. Initial slope mesurements as a function of particle size have been performed under stirring (orthokinetic coagulation) and non-stirring (perikinetic coagulation) conditions. The results, processed for both model

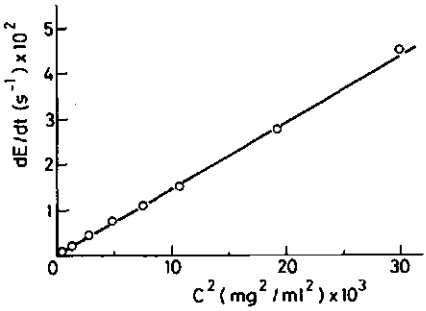

FIGURE 5.8. Rate of coagulation (expressed as the initial value of dE/dt) vs. the square of the sol concentration. Measurements were performed at pH 4 with sol A.

assumptions are shown in fig. 9. As expected [40, p. 444], the rate of coagulation increases with particle size if the sol is stirred. That even in non-stirred sols a definite size effect is observed might be attributed to convection remaining after homogenisation. However, absolute k_{11} values for "perikinetic" coagulation are lower then the Von Smoluchowski value.

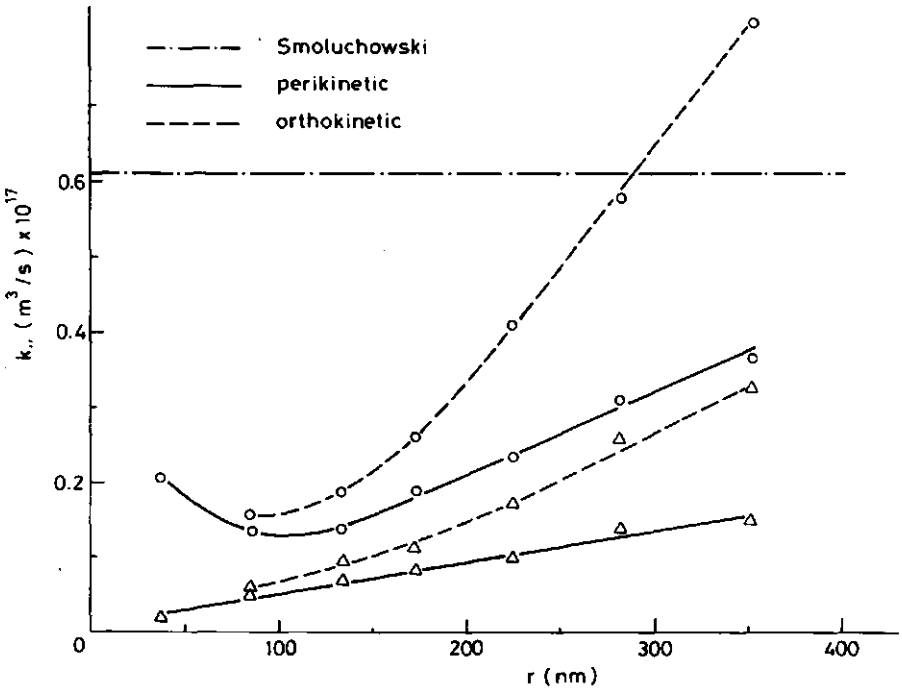

FIGURE 5.9. Rate constant for dimer formation k_{11} vs. particle radius calculated according to model (1) (Δ) or (2) (O). Experimental results obtained for perikinetic (——) and orthokinetc (----) conditions have been incorporated, together with the von Smoluchowksi value (-·-·-·). Values have been obtained at pH 4.

5.5 DISCUSSION

5.5.1 General considerations

In the course of stability investigations performed throughout many years, the awareness grew that the behaviour of a colloidal system is not ruled by one ubiquituous law, but that it is very sensitive to the intrinsic properties of the particles under study. The barrier concept and the assumption of irreversible coagulation might satisfactorily describe the stability of small gold particles, but they do not explain the behaviour of micron sized latex sols, where secondary minimum coagulation is predominant. In addition, virtually no system used for model studies suits the idealized requirements of the theory concerning particle shape and surface structure. Evidence is accumulated that latex particles, whose perfect sphericity attracted many investigators, possess a hairy surface structure [33,34] whereas colloidal metals and oxides have an irregular or porous surface, showing properties and structures different from the bulk material [18,35]. As stability is determined by short range forces between approaching particles, such imperfections might play a major role in the coagulation process. Therefore, every fundamental study concerning "model systems" has to be interpreted in the light of such experimental restrictions.

Though in theoretical studies dealing with colloid stability, coagulation is always considered as a one direction process, there is plenty of evidence that repeptisation is the rule rather then the exception. Also the haematite sols used for the studies reported in this paper showed repeptisation after release of coagulation conditions. Repeptisation even was an important step in the purification of the synthesized sols [16], and resulted for all particle sizes in virtually complete monomer formation [17]. This reversibility indicates that coagulated particles do not come into close contact [22,36]. Whether an equilibrium distance (c in fig. 2) due to secundary minimum coagulation, or a distance of closest approach (b) in the case of primary minimum coagulation has to be considered, will depend on particle size.

For a more quantitative approach of stability phenomena and the influence of distance restrictions on coagulation behaviour according to the theory outlined in the introduction, proper values have to be chosen for the Hamaker constant A, the Stern potential Ψ_d, and the Stern layer thickness Δ.

Calculated A values for haematite in water of 4.5×10^{-20} J have been reported [37,38]. As the true Hamaker constant for water might be somewhat underestimated in the underlying theories [39], this value is probably too high. We therefore adapted $A = 4 \times 10^{-20}$ J in our calculations. A reasonable value for Ψ_d under coagulation conditions, as indicated by electrophoretic measurements, is 30 mV and Δ is of the order of magnitude of a few tenths of a nm. According to fig. 2, a sol is stable if V_{min} (I) is too small to cause secundary minimum coagulation and $V_{min} + V_{max}$ (II) is too high to allow primary minimum coagulation. If an arbitrary value of 5 kT is chosen to classify a system as coagulated or dispersed, stability diagrams can be constructed based on the theory outlined before. In these diagrams, the combination of particle size and electrolyte concentration meeting this criterion can be depicted. Secundary minimum coagulation occurs if I > 5 kT, and primary minimum coagulation if the two conditions II < 5 kT and III > 5 kT are met. In fig. 10, calculated stability diagrams have been constructed for three different values of Δ. They show the 1-1 electrolyte concentrations as a function of particle size for which energies I, II or III equal 5 kT. As with increasing Δ the depth of the primary minimum III decreases drastically, primary minimum coagulation, determining the stability of, in particular, small particles becomes less important. For $\Delta = 0.5$ nm, secundary minimum coagulation predominates for all particle sizes. Besides the magnitude of Δ, Ψ_d has a pronounced influence on the course of the stability trajectories as examplified in fig. 11. A slight change in the Stern-potential value has pronounced effects on the stability-determining mechanisms.

In the present calculations, many assumptions and to a certain extent arbitrary parameter choices have been made. Other values for the energetic criterion, A, Ψ_d and Δ will change the quantitative picture significantly. However, they will not affect the qalitative results of the analysis proposed. One of those results is that the existence of a distance of closest approach (originating in hydration forces or surface contaminants, as suggested in chapter 4) might explain why the c.c.c. decreases with increasing particle size even for small particles for which primary minimum trapping is expected to be predominant, though it is no prerequisite. To illustrate the last mentioned feature, in fig.12, a hypothetical stability diagram is drawn, together with the c.c.c. vs. particle size curve, for five imaginary sols. According to fig.12 the general behaviour of fig.6 can be explained as

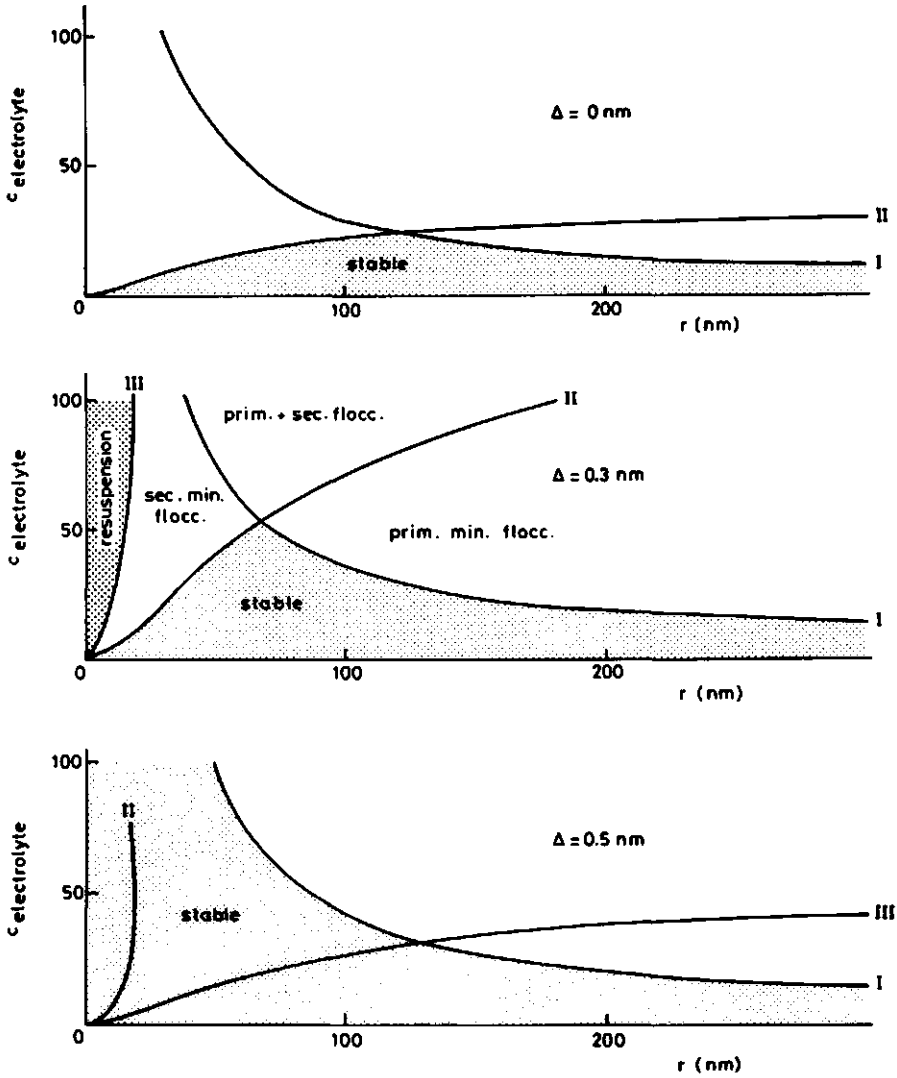

FIGURE 5.10. Influence of the distance of closest approach on the stability of homodiperse spherical sols. The numbers refer to the energy levels given in figure 2, determining secundary minimum coagulation (I), primary minimum coagulation (II) and resuspension (III). Values for Ψ_d and A have been chosen to be 30 mV resp. 4×10^{-20} J.

follow: The sol containing the smallest particles (sol 1) coagulates in the primary minimum, sols 2 and 3 coagulate in the secundary minimum whereas for sols 4 and 5 deviations from the predicted course occur due to the contribution of shear effects, as will be explained below.

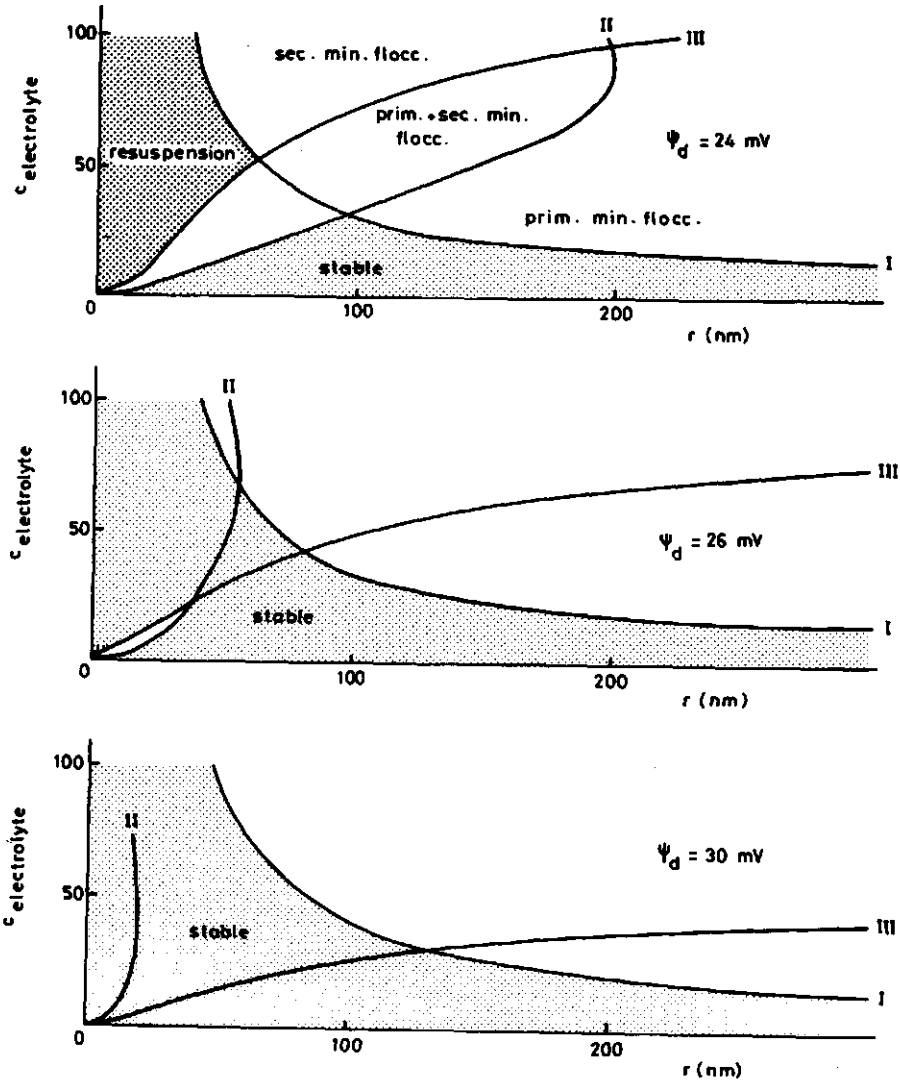

FIGURE 5.11. Influence of the Stern layer potential on the stability of homodisperse sols. Values for A and Δ have been chosen to be 4×10^{-20} J and 0.5 nm. resp.

Redispersion not only occurs if the conditions are altered in such a way that changes in double layer structure favour particle repulsion. By applying moderate shear, repeptisation could be observed even in coagulating systems. Apparently, for the sols under consideration, the forces involved in particle trapping are comparable in magnitude with shear forces exerted

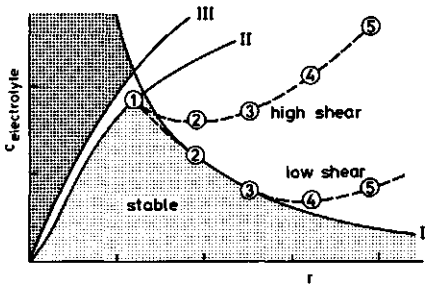

FIGURE 5.12. A hypothetical stability diagram. In this diagram the dependence of the c.c.c. on particle size has been incorporated for five imaginary sols. Sol 1 coagulates due to trapping in the primary minimum, sols 2-5 in the secundary minimum. For bigger particle sizes the behaviour deviates from the predicted size dependence (curve I) due to shear effects. The meaning of the curves I,II and III is explained in fig. 5.10.

on the particles in the process of sample homogenisation. The shear force, a particle at the boundary of a (much) larger aggregate is subjected to, is approximately related to the particle cross section and to the shear stress $\phi = \eta\ dv/dt$ applied. Therefore, the disruption force F_h exerted on a particle of an aggregate can be approximated by

$$F_h = i\ r^2\ \phi \qquad (5.14)$$

where i is a dimensionless geometrical constant. Apparently F_h, and therefore the rate of redispersion, depends strongly on monomer size, i.e. aggregates of large monomers are more vulnerable to redispersion and less stable than aggregates of small ones. On the other hand, the depth of the secondary minimum increases linearly with particle size, thus enhancing instability and retarding resuspension. As the influences of hydrodynamic effects and the secundary minimum are antagonistic, it will depend on their relative magnitude, and therefore on particle size, which one dominates. For small monomers, shear effects are of relatively little importance whereas for bigger ones they will contribute significantly. In order to compensate the consequences of shear, the trapping energy has to be increased by increasing the electrolyte concentration. This explains the in first instance unexpected increase of the c.c.c. with particle size (fig. 6,12) for larger particles. An unambigious proof of this explaination could be obtained by performing coagulation experiments at different, defined shear rates. High shear rates should cause a more pronounced minimum at smaller sizes as is illustrated in fig. 12. However, the equipment used throughout the investigations was not suited for such a systematic study.

Another direct consequence of shear is that the dependence of the slope of the stability curves (log W vs. log c) on particle size will not follow the predictions of the theory. For perikinetic coagulation, the theoretical

size dependence is counteracted by shear. In fact, convection is a potential cause for the lack of concordance between theory and experiment observed in literature.

The pH dependence of the coagulation behaviour of the small particle containing sol is a matter of particular interest, as in the light of the stability theory it exhibits some pecularities. The increase of maximum coagulation velocity if the pH deviates from the pH_0 is not accounted for by the Fuchs theory, which predicts that the rate constant for rapid coagulation is determined by the attractive energy between two particles (see eqn. (10)). As V_A is originated in the van der Waals forces, k_r should be pH independent. Any guess about the cause of the striking pH influence is speculative: As pointed out in a previous report [18] there is some evidence that the surface structure of the haematite under investigation is pH sensitive. Structural changes will modify the close vicinity of the particles, for example by developing hydrous amorphous structures and will influence the parameters which determine the stability of the colloids. As illustrated before, slight alterations in the effective distance of closest approach (b) have a large effect on the stability. Depending on the accessibility and rigidity of, and the charge distribution in the induced surface layer, the electrolyte concentration too might exert influence on its thickness.

Another feature of the curves is that the coagulation rate shows a maximum as a function of the electrolyte concentration. This behaviour is readily explained if primary minimum coagulation occurs for the smallest particles, but at the same time, trapping energy III is too small to enable 100% cagulation efficiency (which will be the case if it is comparable with the barrier energy II). Any increase in electrolyte concentration will reduce the ratio III/II and therefore the coagulation efficiency.

Literature values for the rate constant for rapid coagulation are of the order of $2\text{-}3\times10^{-18}$ m^3s^{-1} [12,28-31] which coincides with our results based on the coalescing sphere approximation (see fig. 9). As in an earlier report [18] it has been shown that deviation from spherical symmetry does not influence the scattering properties of the haematite particles to a large extent, the coalescing sphere approximation might be suitable for practical purposes though its principles are in doubt. The ratio of the probability of a collision induced by a velocity gradient originating from mechanical agitation (like stirring) to the collision probability due to Brownian motion

has been shown to be proportional to r^3 [40]. The enhancement of the coagulation rate due to mechanical agitation will therefore overcompensate the retardation caused by shear induced repeptisation ($\approx r^2$), as shown in fig. 9. Therefore k_{11} increases with particle size.

5.5.2 Some geometrical considerations

Hitherto, all arguments have been based on the assumption that the particles used as model systems can be considered as perfect spheres. However, scanning electron micrographs have shown [17] that the monocrystalline haematite particles rather exhibit the morphological features of rounded off cubes (see chapter 3). Geometrical anisotropy will have some effect on the coagulation behaviour of the sols if reorientation and therefore (size dependent) inertia becomes important. A rigorous approach of the kinetics of interaction of particles with shapes deviating from sphericity is not possible because of the complexity of the underlying theory. However, with some simplification an first impression can be gained:

The effects of geometrical anisotropy, in combination with particle size, on colloid stability is illustrated by a model which considers the interaction of a cube with side ℓ with a flat plate (see fig. 13). The cube is oriented in such a way that the perpendicular line through two of its planes is always parallel to the surface of the plate. So possible rotation of the cube is restricted to one axis. Furthermore, only interactions between the plate and the planes facing toward the plate (shaded dark) are taken into account. For the calculation of the attractive energy, the plate as well as the cube are considered to be infinitesimal bodies. Edge effects are neglected.

For the calculation of interaction energies between two spheres, Derjaguin considered the spheres to consist of concentric rings with parallel planes whose interactions are mathematically accessible [41,42,40]. Following his approach, the cube- plane interactions can be obtained by dividing the plate-faced planes into parallel strips (see fig. 13), reducing the whole problem to the sum of a number of simple flat plate interactions.

The total energy of repulsion or attraction is determined by the individual contributions of the cube planes 1 and 2:

$$V(h,\theta) = V_1(h,\theta) + V_2(h,\theta) \qquad (5.15)$$

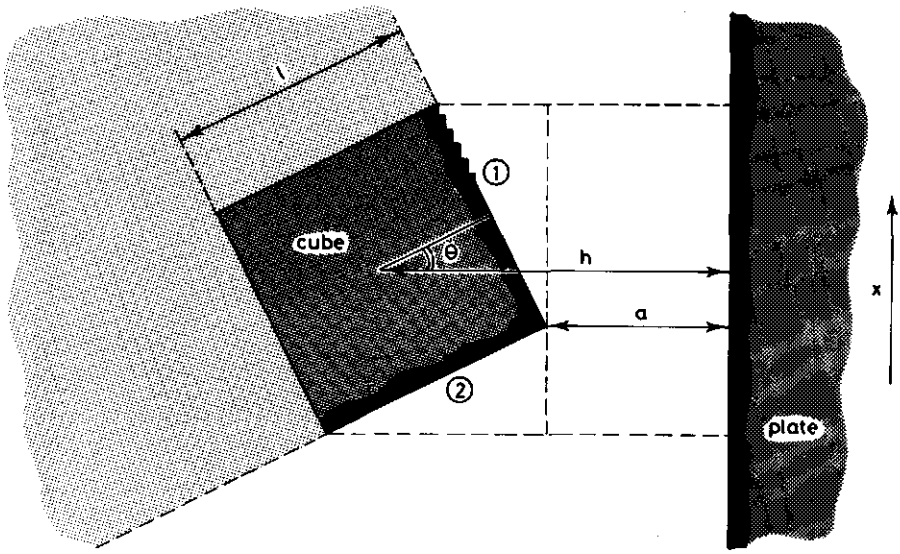

FIGURE 5.13. Schematic representation of the plate-cube interaction model defined in the text. h = plate-cube centre distance. θ = angle of rotation, ℓ = cube side length. 1 and 2: cube planes whose interaction with the plate are accounted for by the model.

In this approach, for the two terms on the right hand side the following expressions apply:

$$V_1(h,\theta) = \int_0^{\ell \cos\theta} V_x\,(a + x\,\mathrm{tg}\theta)\,\ell\,dx \qquad (X = A \text{ or } R) \qquad (5.16)$$

and

$$V_2(h,\theta) = \int_0^{\ell \sin\theta} V_x\,(a + x/\mathrm{tg}\,\theta)\,\ell\,dx \qquad (X = A \text{ or } R) \qquad (5.17)$$

The double layer repulsion $V_R(h)$ between two parallel plates on a distance h, expressed per unit of surface area equals

$$V_R(h) = \xi\, e^{-\kappa h} \qquad (5.18)$$

Here, ξ is $64\,R\,T\,c\,\kappa^{-1}\,\gamma_d^{\,2}$, and $\gamma_d = \tanh(z\,e\,\Psi_d/4\,K\,T)$.

For the attractve case, expressions similar to eqs. (16) and (17) are valid except for the fact that the repulsion energy $V_R(h)$ has to be replaced

by $V_A(h)$, the attraction energy between two flat plates, given by

$$V_A(h) = A/12\ \pi\ h^2 \qquad (5.19)$$

The equations (16) and (17) are solved relatively easily for the repulsive and attractive case by substitution of the equations (18) or (19) in (16) and (17) so that expressions for $V_R(h,\theta)$ and $V_A(h,\theta)$ can be derived for $\theta = 0°$ and $\theta = 45°$:

$$V_R(h,45) = -2\ q/\kappa\ [-1 + \exp(-\kappa\ \ell/2^{\frac{1}{2}})] \qquad (5.20)$$

$$V_R(h,0) = \ell^2\ \xi\ \exp(-\kappa\ h) \qquad (5.21)$$

q being $\xi\ \ell\ \exp\ [-\kappa\ (h-1/2^{\frac{1}{2}})]$ and

$$V_A(h,45) = \ell\ A/(6\ \pi)\ [h^{-1} - (h\ -\ell/2^{\frac{1}{2}})^{-1}] \qquad (5.22)$$

$$V_A(h,0) = -\ell^2\ (A/12\ \pi)\ h^2 \qquad (5.23)$$

For sake of clarity, in the previous analysis, the thickness of the Stern layer has been chosen to be 0. However, in analogy with the theory given for spheres, the Stern layer concept is easily incorporated.

Fig. 14 shows a stability diagram for secundary minimum coagulation for particles having two orientations ($\theta = 0°$ and $\theta = 45°$) under the following conditions: $A = 4x10^{-20}$ J, $\Psi_d = 30$ mV, $\Delta = 0.5$ nm and the stability criterion equals 5 kT. The drawn lines give the coagulation value vs. the size of

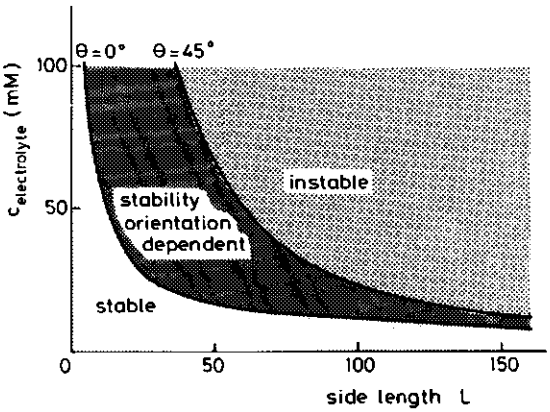

FIGURE 5.14. Stability diagram for two selected cases of the cube-plane interaction: The angle of rotation has been chosen to be either 0 or 45°. Model parameters: $\Psi_d = 30$ mv, $\Delta = 0.5$ nm, $A = 4x10^{-20}$ J. Only secundary minimum coagulation has been accounted for.

cubic particles for the two indicated orientations. The very pronounced angle dependence is obvious. Parallel oriented particles are the less stable ones.

However, whether in actual cases orientational effects will exert any influence on stability will strongly depend on the rotational mobility of the particles in relation to the duration of the collision process. To get an impression about the respective magnitudes, some simple calculations might be useful: If we consider the translation to be determined by Brownian motion, then the collision time, which is the average time needed for the particles to travel through the thickness of the double layer is given by

$$t_{Brown} = [(1/\kappa)^2/2\ D] = 3\pi\ \eta\ r/\kappa^2\ k\ T \qquad (5.24)$$

For particles of 250 nm, in electrolyte solutions varying in concentration from 10^{-3} to 10^{-1} M (coagulation range), $t_{Brown} \approx 10^{-5} - 10^{-7}$ s. At short distances, a cubic particle in the vicinity of the plate is subjected to a torsion exerted by the difference in energy between individual orientations. The maximum driving energy difference for rotation E_R is given by the difference in the total interaction energy $V_t(h,\theta)$ (= $V_A(h,\theta) + V_R(h,\theta)$) between $\theta = 0°$ and $\theta = 45°$:

$$E_R = V_t(h,0) - V_t(h,45) \qquad (5.25)$$

Due to the torsion, the particle can be considered to be a harmonic oscillator with oscillation frequency υ. If the oscillation is undamped and if the oscillation force depends linearly on θ, then

$$E_R = \int_0^{45} B\ \theta\ d\theta = \tfrac{1}{2}\ B^2\theta \qquad (5.26)$$

where B is the torsion constant. As E_R can be calculated from the above theory, B is known. If the moment of inertia J of a cube with side ℓ is chosen to be equal to the moment of inertia J of a sphere with equal weight, the oscillation frequency can be calculated from the equation:

$$2\ \pi\ \upsilon = (B/J)^{\frac{1}{2}} \qquad (5.27)$$

For given values of Ψ_d and r, ν depends on the distance of approach. For

Ψ_d = 30 mV and r = 250 nm, υ is in the order of magnitude of $10^6 - 10^7$ s^{-1}. The number of possible oscillations (j) within the collision time, which is a measure of the reorientation probability, is therefore of the order of unity. If j >> 1 then complete reorientation within the time scale of collision is possible, if j << 1, particles behave like rigid entities with respect to rotation. As υ depends more strongly on particle size then the rate of translation, the outcome might be that small particles reorientate completely in the course of approach, whereas bigger particles do not. For bigger particles, the coagulation efficiency will be lower and therefore a higher electrolyte concentration is needed to ensure maximum coagulation. So in principle, besides shear, particle anisotropy is a potential cause for the observed particle size dependence of the c.c.c.

Regarding shape effects, some additional remarks can be made. Model calculations performed by Czarnecki et.al. [43,44] have shown that surface roughness plays a major role in the determination of the stability of colloid systems and that the dimensions of surface protrusions in relation to the (rotation) mobility of a sphere approaching a rough half space determines the stability. The particles studied in the present report certainly exhibit some degree of roughness, and might even possess some energetic heterogeneity originated in their monocrystalline nature. Roughness as well as heterogeneity will without doubt also contribute to some extent to the observed size effects. To discriminate between all these individual contributions, more sophisticated methods then used in the described experiments are needed, involving particles with different geometry and an experimental set up which allows measurements under controlled shear conditions.

5.6 CONCLUSIONS

In this report we tried to add some new aspects to the problem of colloid stability, both from an energetic as from a kinetic point of view. The arguments given show that the basic concepts of the DLVO theory do explain the observed stability behaviour. However, a distance of closest approach of the particles of the order of a hydrated ion diameter has to be incorporated and effects originating in shear and geometrical anisotropy might superimpose further contributions to the classical behaviour, altering the final picture considerably. By incorporating these effects in the D.L.V.O. approach, many observed trends can be explained:

- The involvement of shear in the coagulation process explains why the expected dependence of stability on particle size is not observed. In addition, it provides arguments for the minimum in the dependence of the critical coagulation concentration on particle size.
- A distance of closest approach which might result from "hydration forces", the presence of irregularities or undefined surface structures accounts for the resuspension of the sols at rather moderate shear rates. Furthermore it offers an explaination why the dependence of the stability ratio on particle size, predicted by theory, is not observed.

Simple calculations show that deviations from sphericity might explain some of the observed effects as well.

In summary, it may be concluded that the experimental trends often encountered in literature rather reflect the specific characteristics of the system under investigation then general trends included in stability theory.

5.7 REFERENCES

(1) Derjaguin, B.V., and Landau, L.D., Acta Physicochim. URSS **14**, 633 (1941).

(2) Verwey, E.J.W., and Overbeek, J.Th.G., "Theory of the Stability of Lyophobic Colloids", Elsevier, Amsterdam, New York (1948).

(3) Reerink, H., and Overbeek, J.Th.G., Discuss. Faraday Soc. **18**, 74 (1954).

(4) Ottewill, R.H., and Shaw, J.N., Discuss. Faraday Soc. **42**, 154 (1966).

(5) van Arkel, A. E., and Kruyt H., R., Recl. Trav. Chim. Pays-Bas **39**, 656 (1920); **40**, 169 (1921).

(6) Iler, R.K., "The Chemistry of Silica", John Wiley & Sons Inc., New York, 382 (1979).

(7) Matthews, B.A., and Rhodes, C.T., J. Colloid Interface Sci. **28**, 71 (1968).

(8) Watillon, A., and Joseph-Petit, A.M., Discuss. Faraday Soc. **42**, 143 (1966).

(9) Ottewill, R.H., and Shaw, J.N., Discuss. Faraday Soc. **42**, 154 (1966).

(10) Kotera, A., Furusawa, K., and Kudo, K., Kolloid-Z. Z. Polym. **240**, 837 (1970).

(11) Wiese, G.R., and Healy, T.W., Trans. Faraday Soc. **66**, 490 (1970).

(12) Gedan, H., Lichtenfeld, H., and Sonntag, H., Colloid Polym. Sci. **260**, 1151 (1982).

(13) Matijević E., Pure Appl. Chem. **50**, 1193 (1978).

(14) Matijević, E., Accounts Chem. Res. **14**, 22 (1981).

(15) Overbeek, J. Th. G., Advan. Colloid Interface Sci. **15**, 251 (1982).

(16) Penners, N.H.G., and Koopal, L.K., Colloids and Surfaces, submitted.

(17) Penners, N.H.G., and Koopal, L.K., Colloids and Surfaces, submitted.

(18) Penners, N.H.G., Lyklema, J., and Koopal, L.K., to be submitted.

(19) Lyklema, J., and de Wit, J.N., Colloid and Polym. Sci. **256**, 1110 (1978).

(20) Bell, G.M., Levine, S., and Mc. Cartney, L.N., J. Colloid Interface Sci. **33**, 335 (1970).

(21) Schenkel, J.H., and Kitchener, J.A., Trans. Faraday Soc. **56**, 161 (1960)

(22) Overbeek, J.Th.G., Colloid and Interface Sci. Vol. I., Kerker, M., Zettlemoyer, A.C., Rowell, R.L., ed., Academic Press, New York (1977).

(23) von Smoluchowski, M., Z. Phys. **17**, 557 (1916); Z. Phys. Chem. **92**, 129 (1917).

(24) Fuchs, N., Z. Phys. **89**, 736 (1934).

(25) Derjaguin, B.V., and Muller, V.M., Dokl. Akad. Nauk S.S.S.R. (Engl. transl.) **176**, 738 (1967).

(26) Spielman, L.A., J. Colloid Interface Sci. **33**, 562 (1970).

(27) Honig, E.P., Roeberson, G.J., and Wiersema, P.H., J. Colloid Interface Sci. **36**, 97 (1971).

(28) Lichtenbelt, J.W.Th., Pathmamanohavan, P., and Wiersema, P., J. Colloid Interface Sci. **49**, 281 (1974).

(29) Hatton, W., Mc Fadyen, P., and Smith, A., J. Chem. Soc., Faraday Trans. 1 **70**, 655 (1974).

(30) Lips, A., Willis, E., J. Chem. Soc., Faraday Trans. 1 **69**, 1226 (1973).

(31) van der Scheer, M., Tanke, A., and Smolders, C., Faraday Discuss. Chem. Soc. **65**, 264 (1978).

(32) Lips, A., Smart, C., and Willis, E., Trans. Faraday Soc. **67**, 2979 (1971).

(33) van der Put, A., thesis, Agricultural University Wageningen, The Netherlands (1980).

(34) Bensley, C.N., and Hunter, R.J., J. Colloid Interface Sci. **92** 448 (1983).

(35) Parks, G.A., and de Bruyn, P.L., J. Phys. Chem. **66**, 967 (1962).

(36) Frens, G., and Overbeek J. Th. G., J. Colloid Interface Sci. **38**, 376 (1972).

(37) Fowkes, F.M., Ind. Eng. Chem., Fundam. **56**, 41 (1964).

(38) Gregory, J., Advan. Colloid Interface Sci. **2**, 396 (1969).

(39) Ninham, B.W., and Parsegian, V.A., J. Chem. Phys. **52**, 4578 (1970).

(40) Hiemenz, P.C., "Principles of Colloid and Surface Chemistry", Lagowski, J.J., ed., Marcel Dekker Inc., New York, 444 (1977).

(41) Derjaguin, B.V., Kolloid. Z. **69**, 155 (1934); Acta Physicochim. URSS **10**, 333 (1939).

(42) Hogg, R., Healy, T.W., and Fuerstenau, D.W., Trans. Faraday Soc. **62**, 1638 (1966).

(43) Czarnecki, J., J. Colloid Interface Sci. **98**, 590 (1984).

(44) Czarnecki, J., Z. Phys. Chem, to be published.

(45) Pashley, R.M., J. Colloid Interface Sci. **80**, 153, (1981).

(46) Pashley, R.M., J. Colloid Interface Sci. **83**, 531 (1981).

(47) Pashley, R.M. and Israelachvili, J.N., J. Colloid Interface Sci. **97**, 446 (1984).

VI. GENERAL REFLECTIONS AND SUGGESTIONS FOR FURTHER RESEARCH

6.1 General

While reading the previous chapters, the reader will have become aware of an important fact: though recently the theories dealing with colloid stability have been in a constant move and new concepts like ion condensation and hydration, being worth further elaboration are suggested for incorporation in existing approaches [1-3], the pitch of the matter in this thesis are experiments and their interpretation in the light of the classical DLVO theory. Within the limits set by the turbidimetric approach and the rather queer nature of the model oxide with regard to its surface properties, the theory explains all trends satisfactorily if reversibility and shear are also taken into account. The approach might occur phenomenological and in some respects ad hoc. However, refinements demand further elaboration of some of the encountered trends which were not accessible in the course of the present study. In particular, extention of stability measurements requires more suphisticated equipment based on single particle detection rather than on a turbidity approach. In addition, the equipment should allow the performance of size dependent measurements at different shear rates. Such a device is at present being constructed in the group of Physical and Colloid Chemistry of the Agricultural University Wageningen.

Chapter 4 points to the complexity of the charging mechanism and the charge distribution at the haematite surface. Though intended to provide unambiguous double layer information, the electrochemical characterisation asks more questions than it solves regarding the charging properties of haematite and maybe oxides in general. Potentiometric titrations are a powerfull tool for unravelling surface properties, but they cannot provide in a comprehensive picture of all surface events. Additional information, obtained by electrokinetic measurements is therefore needed. Due to the obvious restricted nature of streaming potential methods which only apply for heated surfaces, there is a need for the evaluation of the electrokinetic properties of pristine particles by means of micro electrophoresis. A lot of effort, not reported in this thesis, has been put in such experiments using standard equipment (Rank Brothers, Mark II Micro Electrophoresis Device). However, obtaining results proved to be an arduous task, the data found were badly reproducible and the iso electric points considerably lower

then expected from stability- and σ_0 (pH) curves. The cause for such erratic haematite behaviour which has also been observed by many other investigators (see chapter 4) could not be traced. It might be connected to a phenomenon observed while searching for possible explanations: when particles are positioned in an electric field they tend to aggregate irreversibly (electrocoagulation), as is illustrated in figure 1. It shows the turbidity change of an otherwise stable sol in the absence and presence of an electric field whose strength is comparable with the fields applied in electrophoresis.

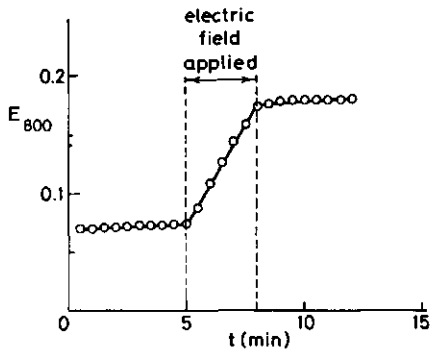

Figure 6.1. Change of the turbidity of a haematite hydrosol (C = 0.012 mg/ml, r = 40 nm) in the absence and presence of an electric field. Field strenth ~ 100 V/m, pH = 5.2, wavelength = 800 nm.

Electrokinetic data, for instance i.e.p. values determined with more sophisticated equipment (Malvern Instruments, Zetasizer II) were in good agreement with the results of the σ_0 (pH) curves. Therefore this instrument seems to be particularly suited for a further investigation of the haematite sols regarding the influence of pH as well as particle size. Unfortunately, except for some preliminary experiments, the Zetasizer II was not available during the project so that an elaboration had to be left for the future.

An other promising source for electrochemical data on oxide surfaces is the use of oxide electrodes. Electrodes, designed according to the procedure outlined in this thesis suffer from certain shortcomings, and it might be a long way, before probes can be designed which fullfill such requirements like reproducibility, short response time and compatibility with colloidal systems. However, the reported results seem to justify such efforts.

On the theoretical side, a lot of work has to be done. Before size effects are really accessible to experimental studies, the influence of surface roughness, dynamics of motion in connection to deviations from spherical shape and surface heterogeneity on stability should be subjected to a

closer investigation. The use of computer simulations to get some grip on these parameters is inevitable.

Finally: the synthesis and the characterisation of the optical and surface (electro)chemical properties of colloidal haematite offered insights in the nature of this oxide representative. Though fascinating, the studies revealed the complexity of the system and consequently sharpened our sense for nuances: With the accumulation of data the awareness grew that our insight in the oxide properties is still restricted and that many additional research is needed. Till then, all attempts to relate stability measurements quantitatively to stability theories are subject to reservations and will inevitably involve parameter assumptions which complicate the allready complex picture of particle interaction even more. Considering these conclusions, haematite as a model system for the investigation of size effects on stability might not have been the most perfect choice from a fundamental point of view. On the other hand however, it is this "imperfection" which destines it as a honourable representative for the vast number of colloids encountered in many applications.

6.2 REFERENCES

(1) Gillespie, T., "The Coagulation of Colloids by Electrolytes", J. Colloid Interface Sci., submitted.

(2) Spitzer, J.J., "A Re-interpretation of Hydration Forces near Charged Surfaces", Nature **310**, 396 (1984).

(3) Hirtzel, C.S., and Rajagopalan, R., "Stability of Colloidal Dispersions", Chem. Eng. Commun., to be published.

LIST OF ABBREVATIONS AND SYMBOLS

DLVO	Derjaguin-Landau-Verwey-Overbeek
R.G.D.	Raleigh-Gans-Debye
SIMULA	computer language, used to perform calculations according to the Mie theory
p.p.z.c.	pristine point of zero charge
c.i.p.	common intersection point
i.e.p.	iso electric point
c.c.c.	critical coagulation concentration
EMF	electro motoric force
M	molarity
G	particle weight
c	concentration
C	sol concentration by weight
N_o	initial particle number concentration
N_t	particle number concentration at time t
t	time
t_i	induction time
$t_{\frac{1}{2}}$	time needed to reduce the particle number in a coagulating system to half its initial value
t_{Brown}	average time needed for particles to travel through two double layer distances due to Brownian motion
T	absolute temperature
r	particle radius
r_o	initial particle radius (nucleus radius)
$r_{E.M.}$	average particle radius, determined by electron microscopy
$r_{L.S.}$	average particle radius, determined by light scattering
k_g	kinetic constant, determining particle growth
k_{11}	rate constant for dimer formation
k_r	rate constant for rapid coagulation
k_s	rate constant for slow coagulation

k	Boltzmann constant
pK	negative logarithm of an equilibrium constant
pH	negative logarithm of the H^+ ion concentration
D	diffusion coefficient
V	molar volume
P	pressure difference applied in streaming potential experiments
p_o	distance parameter in particle attraction equation
n	real refractive index, averaged value
n_ω, n_ε	real refractive indices for a crystallographically anisotropic particle. The index numbers refer to the optical axes of an uniaxial particle.
E_s	streaming potential
τ	turbidity of a colloidal suspension
E_R	torsion energy
V_{max}	highest total interaction energy experienced by particles during approach
V_t	total potential energy of interaction
V_A	attractive interaction energy
V_R	repulsive interaction energy
V_{sec}	secondary minimum interaction energy
W	stability ratio
z	ion valence
e	elementary charge
α	dimensionless size parameter
λ	radiation wavelength or retardation wavelength
κ	absorption coefficient or reciprocal Debye length
κ_{sp}	specific conductance
η	viscosity
σ	surface charge density
$\Delta\sigma$	change in surface charge density
Ψ_d	Stern layer potental
ζ	zeta potential
Δ	Stern layer thickness
ε	dielectric constant = $\varepsilon_o \times \varepsilon_r$

ε_0	dielectric permitivity of vacuum
ε_r	relative dielectric constant
τ	specific turbidity

SUMMARY

Since the foundation of colloid chemistry as a branch of science, much attention has been paid to the subject of colloid stability, i.e. the stability of colloid systems against aggregation. Gradually, our knowledge of the mechanisms involved has improved and models were developed, comprised in the DLVO theory, which form the basis of a quantitative description of the stability of a colloidal system. There is plenty of experimental evidence which substantiate the correctness of the principles of the DLVO theory, and hence, this theory is regarded as one of the fundaments of colloid chemistry. However, in one respect the theory is not confirmed by experiments: calculations predict pronounced size effects, but in practice stability seems to be little affected by particle size.

It was the purpose of this study to gain insight in this contradictory matter. **Chapter 1** offers a more extended introduction to the problem as well as the outline of this study.

Chapter 2 focusses attention on a model system which meets the outlined requirements regarding surface charge, homodispersity, sphericity and particle size range: a method is described for the synthesis of homodisperse haematite (α-Fe_2O_3) sols containing particles whose sizes vary from 35 nm up to 700 nm. This method is principally based on the gradual growth of haematite seeds in supersaturated $FeCl_3$ solutions (heterogeneous nucleation) up to the desired paticle size. As slight deviations in the composition of the growth medium have drastic effects on the shape of the final colloid, emphasize is given to the description of optimal synthesis conditions for spherically shaped particles. Kinetic experiments, performed to unravel the principles of particle growth revealed that the precipitation process is governed by diffusion.

The coagulation experiments described in chapter 5 are monitored by turbidity measurements. Therefore the characterisation of the optical properties of the sols is a prerequisite for further studies. The sols under investigation are homodiperse and contain spherically shaped particles. This makes them particularly suited for such an evaluation, as their scattering behaviour can be interpreted in terms of the Mie theory. Such a comparsion, leading to values for the refractive index (n) and the absorption coefficient (κ) in the wavelength range from 400 to 800 nm is made in **chapter 3.** The agreement between calculations and experiments is good for any wave-

length in the visible range, and for any particle size studied, although the particles are monocrystalline and no perfect spheres.

Any study dealing with electrostatic stabilisation demands some knowledge of the electrochemical behaviour of the system under study. **Chapter 4** pays attention to the electrochemical characterisation of the haematite surface by comparing haematite samples from different origines. In these studies, potentiometric titrations, streaming potential measurements on haematite-coated capillaries and micro electrophoresis were used as the experimental tools to get access to the surface properties. Instead of providing unambiguous data, being valid for all iron oxides occuring in the α-Fe_2O_3 modification, the reported experiments emphasize that the crystal structure of the bulk phase is not the exclusive parameter in determining the electrochemical behaviour of an oxide. The purification procedure, or a heat treatment of the sol (aqueous or dried) plays an important part as well. There is some evidence that the crystal habit of the haematite surface is pH-dependent and that in some cases precipitated amorphous oxide may share in determining the surface properties. Though not going too much into details, the study gives evidence of the fact that the charging mechanisms of haematite are more complicated than expected on the grounds of purely crystallographic considerations.

Inevitably this finding has its impact on the question of colloid stability, which is the dominating item of **chapter 5**. Considering the outcome of the electrochemical study, is it still justified to assume that the haematite particles meet the demands of the stability theory regarding the sharpness of the boundary between bulk material and surrounding liquid? How could a diffuse surface layer be accounted for in existing stability models? Within the restrictions set by such questions, chapter 5 deals with the item of colloid stability with special reference to the influence of particle size on stability: though the value of the critical coagulation concentration depends on particle size and shows a minimum (!), the slopes of the log W - log C plots are virtually size independent. Such trends can be accounted for by the concepts of the DLVO theory, if coagulation reversibility and shear effects are incorporated in the analysis. Deviations from sphericity, which are definitely observed for the systems under investigation, might explain some of the observed effects as is shown by some simple double layer calculations dealing with orientational effects in the interaction of a cubic particle with a half space.

Finally, **chapter 6** reflects on the preceding items and pays attention to its limitations. Furthermore, it points to subjects which deserve further elaboration and mentions the means to make them experimentally accessible.

SAMENVATTING

DE SYNTHESE EN DE STABILITEIT VAN KOLLOIDAAL HOMODISPERS HEMATIET (α-Fe_2O_3)

Zoals de naam reeds suggereert is de kolloidchemie die discipline binnen de scheikunde die zich bezig houdt met de bestudering van het gedrag en de eigenschappen van zgn. kolloiden. Onder kolloiden verstaat men deeltjes die zo klein zijn dat hun bezinking o.i.v. de zwaartekracht slechts een geringe rol speelt. In de praktijk houdt dit in dat de deeltjes meestal kleiner zijn dan 1/1000 millimeter en zich dus zonder geavanceerde mikroskopische hulpmiddelen aan ons oog onttrekken. Dat desalniettemin een hele wetenschapstak gericht is op de bestudering van deze dwergen vindt zijn oorzaak in hun praktisch belang: Verven zijn in principe niets anders dan zeer fijn verdeelde (en dus kolloidale) pigmenten en harsen in organische oplosmiddelen of water. Melk bevat mikroskopisch kleine vetdruppeltjes en eiwit waaraan dit product de kleur en voedingswaarde te danken heeft. Zeep ontleent zijn reinigende werking deels aan het feit dat de zeepmoleculen in water kolloidale klusters vormen waarin verontreinigingen kunnen worden opgenomen. Het vastleggen van muziek op geluidsbanden berust op de magnetisatie van zeer kleine, homogeen op een drager verdeelde oxide deeltjes. Kortom, kolloiden zijn in ons dagelijks leven alomtegenwoordig.

Een vloeistof, waarin grote hoeveelheden kolloidale deeltjes voorkomen (zoals in de bovengenoemde melk of verf) noemt men een sol. De vraag: "Zijn de kolloiden als afzonderlijke deeltjes in de vloeistof verdeeld (zijn ze stabiel), of hebben ze de neiging om samen te klonteren (zijn ze instabiel)?" is voor de eigenschappen van een kolloidaal systeem zoals een sol van groot belang. Is het sol instabiel dan vormen zich klonten (aggregaten) die door hun grootte o.i.v. de zwaartekracht binnen korte tijd bezinken. Geschifte advokaat, zure melk en klonterende verf zijn voorbeelden van instabiele solen. De praktische konsequenties van instabiliteit behoeven geen verdere toelichting. Soms is instabiliteit echter gewenst, bijvoorbeeld bij het verwijderen van fijn verdeelde verontreinigingen uit oppervlaktewater bij de drinkwaterbereiding. Door het gebruik van additieven kan de aggregatie, en dus het zuiveringsproces worden bevorderd. Stabiliteit is kennelijk een belangrijk aspect bij de beheersing van veel processen in de praktijk.

Wil men de stabiliteit beïnvloeden, dan is een gedegen kennis van de factoren die de stabiliteit bepalen een eerste vereiste. Reeds in de veertiger jaren werd een theorie ontwikkeld (de zg. DLVO theorie) die de stabiliteit relateert aan de tussen de kolloidale deeltjes werkzame krachten. Deze krachten kunnen worden opgesplitst in twee komponenten:

- Een attractieve (aantrekkende) komponent, die altijd optreedt als twee deeltjes in elkaars nabijheid komen.
- Een repulsieve (afstotende) komponent, die zijn oorsprong vindt in de lading die vrijwel alle kolloidale deeltjes op hun oppervlak dragen. De mate van afstoting wordt in sterke mate bepaald door de samenstelling van de vloeistof waarin de deeltjes zich bevinden.

Van de balans tussen deze tegengestelde komponenten hangt het af of een sol stabiel is of niet.

Een van de factoren die bepaalt welke komponent overheerst is de doorsnede van de kolloidale deeltjes. De genoemde theorie voorspelt dat onder gelijke omstandigheden kleine deeltjes eerder tot vlokking neigen dan grote. Men heeft dit verband echter nog nooit eenduidig experimenteel kunnen aantonen, zodat binnen de kolloidchemie de kwestie van grootte en stabiliteit nog steeds een discussiepunt vormt. Het was de opzet van dit onderzoek, deze kwestie verder uit te diepen. Omdat de deeltjesdoorsnede in dit onderzoek de belangrijkste variabele was moest het kolloid, waarmee het onderzoek is uitgevoerd, aan twee eisen voldoen:

(I) Alle deeltjes binnen een sol moesten even groot en bolvormig zijn

(II) De grootte van de deeltjes moest over een groot bereik gevarieerd kunnen worden.

Uit praktische overwegingen werd uiteindelijk een bepaalde vorm van ijzeroxide, het zgn. hematiet (α-Fe_2O_3) als modelsysteem gekozen. In de inleiding (**hoodstuk 1**) wordt de systeemkeuze verder toegelicht.

Hoofdstuk 2 handelt over de bereiding van ijzeroxidesolen die aan de bovenstaande vereisten voldoen. Behalve dat de omstandigheden worden beschreven die tot de gewenste resultaten leiden wordt er ook aandacht besteed aan het proces van de deeltjesvorming.

Door de geringe afmetingen van de afzonderlijke kolloidale deeltjes en hun aggregaten zijn speciale technieken nodig om inzicht te krijgen in het vlokproces. Een veelgebruikte methode berust op het verschijnsel dat de lichtdoorlaatbaarheid van een sol verandert met de hoeveelheid aggregaten die in het sol voorkomen. Hoe meer aggregaten er per tijdseenheid worden

gevormd (dus hoe instabieler het sol), des te sterker deze verandering zal zijn. In principe kan dus de verandering van de lichtdoorlaatbaarheid van een sol worden gebruikt als maat voor de stabiliteit. Dit is echter alleen mogelijk als de optische eigenschappen van het stabiele sol in relatie tot deeltjesgrootte, -koncentratie en golflengte van het gebruikte licht bekend zijn. Elke substantie wordt in dit opzicht gekenmerkt door enkele specifieke konstanten. In **hoofdstuk** 3 zijn de resultaten van de optische karakterisering van de modelsolen samengevat. De metingen worden vergeleken met de berekende waarden die volgen uit de Mie- theorie, een lichtverstrooiingstheorie voor bolvormige deeltjes.

Zoals reeds eerder vermeld hangt de stabiliteit van kolloiden in sterke mate af van de elektrische krachten die tussen de deeltjes werkzaam zijn en de beïnvloeding van deze krachten door de samenstelling van de omringende vloestof. **Hoofdstuk** 4 besteedt aandacht aan de oorzaak van de elektische wisselwerkingen: de deeltjeslading. Hoe verandert deze lading met de zuurgraad van het sol en met het zoutgehalte? In welk opzicht verschilt de lading van in principe identieke oxiden die slechts een andere voorbehandeling hebben ondergaan? Dergelijke vragen staan in dit hoofdstuk centraal. De experimenten illustreren het complexe karakter van de mechanismen die de lading van het hematiet bepalen.

Hoofdstuk 5 gaat uiteindelijk in op het verband tussen grootte en stabiliteit. De belangrijkste conclusie uit dit hoofdstuk kan alsvolgt worden samengevat: de voorspellingen van de DLVO theorie worden door de experimenten niet bevestigd. Dit houdt echter niet à priori in dat de theorie op verkeerde beginselen is gebaseerd. Houdt men rekening met het feit dat de aggregaten weer uit elkaar kunnen vallen tot afzonderlijke deetjes (resuspensie) en dat de mate van resuspensie afhangt van de deeltjesgrootte, dan kunnen alle waargenomen effecten binnen het kader van de DLVO theorie worden verklaard. Ook blijken afwijkingen van de bolvorm (die in praktische systemen eerder de regel dan de uitzondering vormen) in belangrijke mate de stabiliteit en het effect van de deeltjesgrootte hierop te kunnen beïnvloeden.

Tot slot plaatst **hoofdstuk** 6 enkele kanttekeningen bij het project. Probleempunten worden aangestipt en suggesties gedaan voor verder onderzoek.

HINTERGRÜNDE DES PROMOTIONSTHEMAS

Die Kolloidchemie ist eine selbstständige Disziplin innerhalb der Physikalischen Chemie, in der das Verhalten und die Eigenschaften sogenannter **Kolloide** erforscht wird. Darunter versteht man Partikel die so klein sind, dass sie unter dem Einfluss der Schwerkraft praktisch nicht sedimentieren. Der Unterschied zwischen kolloidaler und nicht kolloidaler Materie wird also primär durch den Dispersionsgrad im Verhältnis zur Gravitation bestimmt. Wasser z.B. ist als Regentropfen der nicht kolloidalen und in vernebelter Form der kolloidalen Substanz zuzuordnen. In den meisten Fällen sind kolloidale Partikel kleiner als 1/1000 Millimeter und daher nur mit aufwendigen mikroskopischen Instrumenten sichtbar zu machen. Dass sich trotz ihrer unscheinbaren Abmessungen ganze Wirtschaftszweige mit ihnen beschäftigen ist auf ihre ausgesprochen praktische Bedeutung zurückzuführen:

- **Farben** sind Dispersionen sehr kleiner (und demnach kolloidaler) Pigmentpartikel und Harze in einem organischen Lösungsmittel (z.B. Lacke) oder Wasser (z.B. Latex).
- **Milch** enthält mikroskopisch kleine Fetttröpfchen und Eiweisspartikel die sowohl Farbe als auch Nährwert dieses Naturproduktes bestimmen.
- Die Reinigungseigenschaften der **Seife** sind zum Teil zurückzuführen auf die Tatsache dass die individuellen Seifenmoleküle in wässeriger Lösung Aggregate bilden die den Schmutz binden.
- Die Aufnahmeeigenschaften eines Tonbands beruhen auf der Magnetisierung sehr kleiner, homogen auf einem Kunststofband aufgetragener **Metaloxydpartikel.**

Kolloide sind in der Natur, der Industrie und in vielen Bereichen des täglichen Lebens allgegenwärtig. Meistens sind die kolloidalen Partikel in hohen Konzentrationen in einer Flüssigkeit enthalten. Die ersten drei der obengenannten Kolloide sind Beispiele für solche Partikel-Flüssigkeit Gemische die man Sole nennt.

Innerhalb der Kolloidchemie ist die sogenannte **Solstabilität**, die Eigenschaften und Nutzwert eines kolloidalen Systems oft in extremen Masse beeinflusst, eines der zentralen Themen. Ein Sol ist **stabil** wenn sich die kolloidalen Teilchen von einander getrennt in der sie umringenden Flüssigkeit befinden. (siehe Abb.) Neigen die Partikel dahingegen zur Verklebung, dann nennt man das Sol **instabil.** In einem instabilen Sol bilden sich Aggregate die unter dem Einfluss der Schwerkraft innerhalb kurzer Zeit sedimentieren.

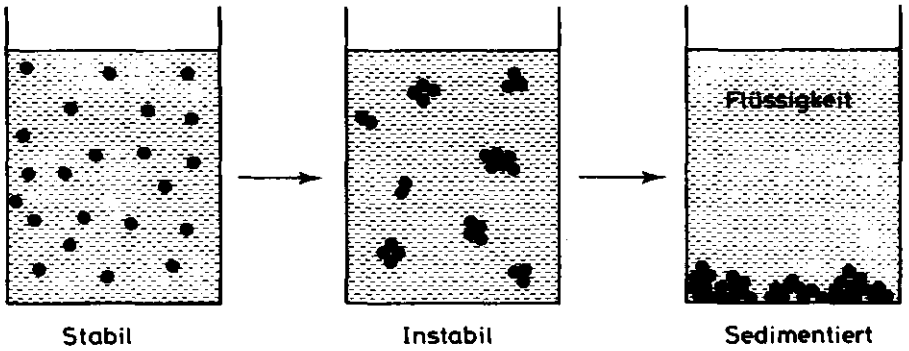

Geronnener Eierlikör, sauere Milch und Klumpenbildung in Farben beruhen auf Instabilität und illustrieren ihre oft negativen Auswirkungen. Für bestimmte Zwecke ist Instabilität jedoch erwünscht, z.B. bei der Entfernung kleiner Partikel (z.B. Kohlestaub) aus verschmutztem Wasser. Die Stabilitätsverringerung wird in diesem Falle erreicht durch den Zusatz bestimmter Chemikalien.

Da die Stabilität scheinbar nicht zu den unabänderlichen Eigenschaften eines kolloidalen Systems gehört, sondern durch bestimmte Eingriffe verändert werden kann, stellt sich die Frage welche Faktoren nun stabilitätsbestimmend sind und wie diese Faktoren die Stabilität beeinflussen. Theoretische Überlegungen führten schon in den vierziger Jahren zu einer Stabilitätstheorie (nach ihren Grundlegern Derjaguin, Landau, Verwey und Overbeek **DLVO Theorie** genannt) die kwantitativ den Zusammenhang zwischen Stabilität einerseits und Teilcheneigenschaften sowie Zusammensetzung der Flüssigkeit andererseits beschreibt. Sie berücksichtigt fast alle experimentellen Wahrnehmungen und hat darum bis heute nichts von ihrer Bedeutung verloren. In einer Hinsicht aber besteht ein deutlicher Gegensatz zwischen den Vorhersagen der DLVO-Theorie und den Ergebnissen experimenteller Forschung: die auf Grund theoretischer Erwägungen erwartete Zunahme der Kolloidstabilität mit zunehmender **Teilchengrösse** wurde experimentell nie eindeutig bestätigt, und hat sich dadurch in mehr als 40 Jahren zu einer der Kernfragen der Stabilitätstheorie entwickelt.

Diese Dissertation versucht zu den Hintergründen dieser Problematik vorzudringen und ihr durch die Integration experimenteller Daten in theoretischen Betrachtungen neue Impulse zu vermitteln. Die Arbeit ist in drei Hauptteile gegliedert:

(I) Modelsolsynthese. Für experimentelle Studien die sich mit den Zusammenhängen zwischen Solstablilität und Teilchengrösse beschäftigen sind Modelsole die kugelförmige, in der Grösse identische Partikel enthalten, unerlässlich. Der erste Teil dieser Arbeit beschäftigt sich darum mit der Synthese solcher Sole deren Kolloidsubstanz aus α-Fe_2O_3 (**Eisenoxyd**) besteht. Die Wahl der Substanz wurde teilweise durch ihre ausserordentliche Relevanz bestimmt: Eisenoxyd ist ein in der Natur weit verbreitetes Mineral, dass in natürlicher Form, aber auch synthetisch hergestellt in vielen Produkten verarbeitet wird; z.B. in Farben, Kosmetikartikel und in Tonbändern. Auch als Korrosionsprodukt (Rost) hat es grosse Bedeutung.

(II) Charakterisierung. Systematische Stabilitätsstudien sind nur dann möglich, wenn die Eigenschaften der Sole und der in ihnen enthaltenen Kolloide bekannt sind. Mit der Bestimmung dieser Eigenschaften beschäftigt sich der mittlere Teil dieser Arbeit.

(III) Stabilität. Die Solstabilität in Abhängigkeit der Teilchengrösse steht im Mittelpunkt des letzten Teiles der Dissertation. Eine Abhängigkeit der Stabilität von der Teilchengrösse, die auf Grund der Vorhersagen der DLVO Theorie zu erwarten ist wurde nicht wahrgenommen. Trotz dieses augenscheinlichen Gegensatzes stimmen Theorie und Praxis weitgehend überein wenn mann die Ausgangspunkte der Theorie den spezifischen experimentellen Gegebenheiten anpasst.

Zusammenfassend kann gesagt werden dass sich die DLVO Theorie auch bezüglich des Einflusses der Partikelgrösse auf die Kolloidstabilität bewährt. Die stabilitätsbestimmenden Mechanismen sind jedoch komplizierter als im allgemeinen angenommen wird und eng verbunden mit den spezifischen Eigenschaften der kolloidalen Substanz.

CURRICULUM VITAE

De auteur van dit proefschrift werd op 19 september 1956 in Selfkant-Wehr (Duitsland) geboren. In 1974 behaalde hij aan het Bisschoppelijk College te Sittard het diploma Atheneum B, en begon in hetzelfde jaar met zijn studie aan de Landbouwhogeschool.

In september 1977 legde hij het kandidaatsexamen moleculaire wetenschappen (chemische orientatie) af. In zijn ingenieursstudie, welke in september 1980 werd afgesloten zijn naast het hoofdvak Fysische en Kolloidchemie de vakken Biochemie en Virologie opgenomen. Zijn stage vervulde hij bij het Polymer Department van het Weizmann Institute of Science (Israel).

Van september 1980 tot november 1984 was hij als wetenschappelijk medewerker in tijdelijke dienst verbonden aan de vakgroep voor Fysische en Kolloidchemie waar hij betrokken was bij het kolloidchemie onderwijs en het in dit proefschrift beschreven onderzoek heeft uitgevoerd.

Vanaf 1 november 1984 is hij als chemicus verbonden aan de afdeling Chemie van het ECN te Petten.

NAWOORD

Een proefschrift is niet slechts het product van de activiteiten van één persoon, de promovendus. Veel mensen, als individu of als groep dragen tot de tot stand koming ervan bij. Reden genoeg, hun bijdragen de revue te laten passeren:

Reeds in de zestiger jaren legden mijn ouders de basis voor mijn verdere ontwikkeling toen zij in wijs vooruitzicht de "Volksschule" verwisselden voor de "Lagere school". En in de jaren die daarop volgden hebben zij door hun voortdurende aandacht en belangstelling veel aan het verdere verloop van mijn opleiding bijgedragen. Monique's betrokkenheid, geduld en nuchtere (soms ook ontnuchterende) kijk op het doen en laten van "haar" promovendus zijn nauw met de promotie verweven. Zij is mij in al die jaren een grote steun geweest.

Ook al is een proefschrift "een proeve van bekwaamheid tot het **zelfstandig** beoefenen van de wetenschap", op kritieke tijden is een gesprek over de gang van zaken onontbeerlijk. Luuk Koopal, begeleider bij uitstek, was altijd beschikbaar, enthousiast, en nooit om een antwoord verlegen. Hans Lyklema ben ik zeer erkentelijk voor zijn interesse en de open houding waarmee hij bij de verschillende stadia van het onderzoek betrokken is geweest. Dat daarbij de promotor en de mens altijd nauw waren verweven is niet de geringste oorzaak voor het feit dat ik met plezier terugkijk op de jaren die ik op het laboratorium voor Fysische en Kolloidchemie mocht doorbrengen.

Erna Rouwendal en Geert Bodewitz hebben nauwgezet een gedeelte van de experimenten voor hun rekening genomen, ook al waren de daarmee verbonden werkzaamheden niet altijd even aantrekkelijk en motiverend.

Geen wetenschappelijk werk zonder geschikte apparatuur en chemicaliën! Dit feit heb ik in de loop van het onderzoek meermaals moeten ervaren. Gelukkig waren er dan Ben Spee en Willem van Maanen, die met hulpvaardigheid en organisatietalent de impasses probeerden te doorbreken (vaak met succes). Waren de problemen van meer technische aard, dan kon ik altijd bij de vaklui Hennie van Beek en Louis Verhagen terecht. Dat deze "Profs" behalve snelle hulp te bieden ook de moeite namen mij ignoramus in de beginselen van hun vak in te wijden weet ik zeer te waarderen.

In een tijd dat ook de chemie niet zonder electronische randapparatuur kan, zijn bekwame electronici een vereiste. Ronald Wegh en Rob Vullings waren altijd wel bereid mij met een glimlach terzijde te staan als een

een vermoeide HP-85 of een recalcitrante roerder het lieten afweten.

Als met experimenteren wordt gestopt dan nemen de werkzaamheden van een promovendus meer administratieve vormen aan. Ideeën en resultaten worden op papier gebracht en uiteindelijk tot een goed ogend manuscript verwerkt. In dit stadium heb ik van Yvonne Toussaint en Wil van der Made veel steun ondervonden, hetzij direct door het typen van delen van dit proefschrift, hetzij indirect door de gezellige sfeer waarmee zij de uren die ik achter de tekstverwerker heb doorgebracht wisten te omkleden. Bert Bouman stond mij altijd met uitgesproken vriendelijkheid en hulpvaardigheid terzijde als het erom ging tot de geheimen van de tekstverwerker door te dringen.

De resultaten in dit proefschrift zijn voor het grootste gedeelte weergegeven in de vorm van figuren, die door Gerrit Buurman bekwaam en kreatief zijn vervaardigd. Hij heeft hiermee in belangrijke mate tot de uiteindelijke vorm van de dissertatie bijgedragen.
Buiten de vakgroep hebben Herman Elerie, Felix Thiel en Bram Boekestein van de afdeling voor Electronenmicroscopie van de TFDL een bijdrage geleverd. De regelmatig terugkerende E.M. sessions hadden in hun aanwezigheid altijd een sfeervol karakter.

Hoe belangrijk en goede werksfeer is zowel voor de voortgang van het werk, als ook voor het plezier dat eraan wordt beleefd behoeft geen toelichting. Alle huidige en voormalige medewerk(st)ers en studenten van de vakgroep voor Fysische en Kolloidchemie hebben ertoe bijgedragen dat ik in dit opzicht niets te klagen heb gehad.

Tot slot wil ik ook nog mijn vrienden (m/v) noemen, die zeer onwetenschappelijk maar o zo wezenlijk tot de totstandkoming van het proefschrift hebben bijgedragen door op gezette tijden voor de nodige afleiding te zorgen.